

Research Article

# The traditional herbal formulation, *Jianpiyifei II*, reduces pulmonary inflammation induced by influenza A virus and cigarette smoke in mice

 Xuhua Yu<sup>1,\*</sup>, Tiantian Cai<sup>1,\*</sup>, Long Fan<sup>1</sup>, Ziyao Liang<sup>1</sup>, Qiuling Du<sup>2,3</sup>, Qi Wang<sup>4</sup>, Zifeng Yang<sup>3</sup>,  Ross Vlahos<sup>5</sup>, Lei Wu<sup>1,†</sup> and Lin Lin<sup>1,†</sup>

<sup>1</sup>The Second Affiliated Hospital of Guangzhou University of Chinese Medicine, Guangzhou 510120, China; <sup>2</sup>Guangdong Key laboratory of Clinical Molecular Medicine and Diagnostics, Guangzhou First People's Hospital, School of Medicine, South China University of Technology, Guangzhou, Guangdong, China; <sup>3</sup>State Key Laboratory of Respiratory Disease, National Clinical Research Center for Respiratory Disease, Guangzhou Institute of Respiratory Health, the First Affiliated Hospital of Guangzhou Medical University, Guangzhou, Guangdong 510180, China; <sup>4</sup>Institute of Clinical Pharmacology, Guangzhou University of Chinese Medicine, Guangzhou 510405, China; <sup>5</sup>School of Health and Biomedical Sciences, RMIT University, Bundoora, VIC 3083, Australia

**Correspondence:** Lin Lin (drlinlin620@163.com)



Chronic obstructive pulmonary disease (COPD) is a worldwide chronic inflammatory lung disease, and influenza A virus (IAV) infection is a common cause of acute exacerbations of COPD (AECOPD). Therefore, targeting viral infections represents a promising strategy to prevent the occurrence and development of inflammatory flare ups in AECOPD. *Jianpiyifei II* (JPYFII) is a traditional herbal medicine used in China to treat patients with COPD, and its clinical indications are not well understood. However, investigation of the anti-inflammatory effects and underlying mechanism using an animal model of smoking have been reported in a previous study by our group. In addition, some included herbs, such as *Radix astragali* and *Radix apleuri*, were reported to exhibit antiviral effects. Therefore, the aim of the present study was to investigate whether JPYFII formulation relieved acute inflammation by clearing the IAV in a mouse model that was exposed to cigarette smoke experimentally. JPYFII formulation treatment during smoke exposure and IAV infection significantly reduced the number of cells observed in bronchoalveolar lavage fluid (BALF), expression of pro-inflammatory cytokines, chemokines, superoxide production, and viral load in IAV-infected and smoke-exposed mice. However, JPYFII formulation treatment during smoke exposure alone did not reduce the number of cells in BALF or the expression of *Il-6*, *Tnf-α*, and *Il-1β*. The results demonstrated that JPYFII formulation exerted an antiviral effect and reduced the exacerbation of lung inflammation in cigarette smoke (CS)-exposed mice infected with IAV. Our results suggested that JPYFII formulation could potentially be used to treat patients with AECOPD associated with IAV infection.

\*These authors have equal contribution as first authors.

†These authors have equal contribution as correspondence authors.

Received: 22 January 2021

Revised: 02 July 2021

Accepted: 08 July 2021

Accepted Manuscript online:  
08 July 2021

Version of Record published:  
27 July 2021

## Introduction

Chronic obstructive pulmonary disease (COPD) is a worldwide chronic inflammatory lung condition characterized by irreversible airflow limitation [1]. Acute exacerbation of COPD (AECOPD) is associated with a range of symptoms, including aggravated coughing, breathing difficulty, sputum production, and wheezing, and it is a leading cause of death in COPD patients [2]. The most recent GOLD report predicted that COPD would become the third highest cause of morbidity and mortality worldwide by 2030 [3]. In China COPD was the fourth leading cause of death in 2017 [4], and the mortality rate of in-hospital patients with AECOPD was 2.5–24.5% [5]. AECOPD accelerates declining lung function and induces numerous additional complications including heart failure, respiratory failure, pulmonary embolism, and pneumothorax, increasing the associated global economic burden annually [6–8].

Smoking and air pollution are the leading causes of COPD [1,9]. AECOPD is characterized by acute inflammatory attack of the lungs, and is triggered by infections with pathogenic microorganisms [10], particularly respiratory viral infections [11]. In patients with AECOPD, the most common viruses in the lung are human rhinovirus, respiratory syncytial virus, and influenza A virus (IAV) [12]. Smoking is a common cause of COPD and can lead to abnormal host responses to viral infections [13,14]. During the current coronavirus disease 2019 pandemic, it has become evident that severe acute respiratory syndrome coronavirus-2 infection increases the risk of severe comorbidities in patients with COPD [15]. In a previous study, cigarette smoke (CS) aggravated inflammatory response in mice infected with influenza A virus [16].

Acute exacerbation of inflammation is one of the main pathological features of AECOPD and involves excessive release of proinflammatory cytokines, excessive oxidative stress, and a protease-antiprotease imbalance [17–19]. A sustained influx of inflammatory cells into the lungs accompanied by overproduction of proinflammatory factors and superoxide leads to increased lung inflammation and injury to airway structure (i.e., small airway collapse and airway obstruction) in the lungs of COPD patients who have been infected with respiratory viruses [12,20,21]. Therefore, inflammation induced by viral infections in lungs exposed to cigarette smoke (CS) is an important target for the prevention and treatment of AECOPD [10]. However, influenza vaccination is the only current recommendation to reduce the risk of hospitalization for virus-related COPD exacerbations [22].

*Jianpiyifei II (JPYFII)* formulation is a traditional herbal medicine used to treat COPD [23]. It is composed of *Radix astragali*, *Rhizoma cimicifugae*, *Radix codonopsis*, *Rhizoma atractylodis macrocephalae*, *Radix bupleuri*, *Herba cynomorii*, *Fructus viticis negundinis*, and *Semen persicae*. Our group has previously reported that *JPYFII* formulation reduced St. George's Respiratory Questionnaire scores and symptom scores in patients with stable COPD [23]. Notably, however, the mechanisms of action of *JPYFII* formulation are not fully understood. It reportedly suppressed lung inflammation via NF- $\kappa$ B signaling pathway in a CS and lipopolysaccharide-induced mouse model [24]. *Radix bupleuri*, a component of the *JPYFII* formulation, has been widely used to treat fever and sore throat caused by influenza virus infection [25,26]. Several small molecules found in *JPYFII* formulation such as quercetin exhibit antiviral effects *in vitro* [27–29], indicating that it may be possible to use *JPYFII* formulation to treat viral infection-related AECOPD.

The present study was conducted to test the hypothesis that *JPYFII* formulation can relieve IAV-associated lung inflammation by clearing the virus in a mouse model of CS and IAV infection. Identification of a herbal formulation that can reduce IAV-induced airway inflammation in CS-exposed mice may have clinical implications for the treatment of AECOPD associated with IAV infection.

## Materials and methods

### Animals

Female BALB/c mice aged of 7 to 9 weeks and weighing 18–20 g were obtained from SPF (Beijing) Biotechnology Co., Ltd. (Beijing, China). All experiments were conducted in the Guangdong Province Engineering Technology Research Institute of Traditional Chinese Medicine, where the experimental center of the Second Affiliated Hospital of Guangzhou University of Chinese Medicine is located. The experiments were performed in compliance with the guidelines of the National Health and Medical Research Council in China and were approved by the Animal Ethics Committee of Guangdong Province Engineering Technology Research Institute of Traditional Chinese Medicine (GDPITCM160129).

### CS exposure

Mice were exposed to smoke produced by burning filter-tipped DaQianMen cigarettes (Shanghai Tobacco Group Co., Ltd., Shanghai, China) using an 18-L plastic chamber in a class II biosafety cabinet as previously described [30]. CS was generated in a 60-ml tidal over 10 s to mimic human smoking inhalation volume and the typical burn rate of cigarette. Mice received smoke from nine cigarettes per day for 4 days using a protocol in which mice were exposed to CS for 1 h, three times per day at 9 a.m., 12 noon, and 3 p.m. Smoke generated in the chamber exhibited a total suspended particulate mass concentration at 540 mg.m<sup>-3</sup>. Sham-exposed mice were placed in an 18-L plastic chamber but did not receive CS. Commercially available filter-tipped DaQianMen cigarettes with the following composition were used: 11 mg or less of tar, 0.8 mg or less of nicotine, and 13 mg or less of CO.

**Table 1** The components of *JPYFII* formulation

Voucher No.	Plant Latin name	Weight (g)	Family	Used part
160717	<i>Radix Astragali</i>	500	Leguminosae	Root
160718	<i>Rhizoma Cimicifugae</i>	167	Ranunculaceae	Rhizome
160719	<i>Radix Codonopsis</i>	500	Campanulaceae	Root
160720	<i>Rhizoma Atractylodis Macrocephalae</i>	250	Asteraceae	Rhizome
160721	<i>Radix Bupleuri</i>	167	Umbelliferae	Root
160722	<i>Herba Cynomorii</i>	250	Cynomoriaceae	Whole plant
160723	<i>Fructus Viticis Negundinis</i>	250	Verbenaceae	Fruit
160724	<i>Semen Persicae</i>	167	Rosaceae	Seed

## IAV infection

After CS or sham exposure for four days, mice were anesthetized with isoflurane on day 5 and given 12 plaque-forming units (PFU) of A/PR/8/34 (H1N1) influenza virus (provided by Professor Zifeng Yang, Guangzhou Institute of Respiratory Health, Guangzhou, China) via nasal aspiration in 30  $\mu$ l of minimal essential Eagle's medium (MEM) as previously described [16,31]. An equal volume of MEM was administered intranasally to vehicle-control mice. The mice were then culled 3 or 5 days after viral infection. Changes in body weight, an indicator of infection severity, were recorded daily.

## *JPYFII* formulation preparation and treatment

*JPYFII* formulation is a combination of eight Chinese herbal medicines. *JPYFII* formulation was prepared as previous described [24]. In brief, eight certified dried herbal medicine were purchased from the Second Affiliated Hospital of Guangzhou University of Chinese Medicine (Table 1), powdered and extracted twice in ten times their volume of boiling water for 90 min. Each water extract was filtered and dehydrated under a vacuum. The residues were freeze-dried and stored in at 4°C prior to use. The extract solution was freshly prepared daily by dissolving of 1.6 g freeze-dried powder into 1 ml of saline for 30 min and using ultrasonic dissociation to assist dissolving. Syringe filters with a pore size of 0.45  $\mu$ m were used to remove any bacteria and insoluble powder before the mice were gavaged with the solution. The main compounds included in the formulation were analyzed and identified via liquid chromatography-mass spectrometry as previously described [24].

Oral gavage of *JPYFII* formulation (24 g/kg) was completed before 8 a.m. daily, which was 1 h before the first CS exposure or IAV infection. The mice received *JPYFII* formulation until they were assessed on day 5 post-infection. The *JPYFII* formulation dose used was based on results obtained from anti-inflammatory dose screening in an IAV-induced CS model (Supplementary Figure S1). It was determined that the 6.7 g/kg body weight of mice was equivalent to a typical dose for humans after conversion based on body surface area. In a separate study, treatment with *JPYFII* formulation was performed in the first 4 days during CS exposure and stopped before IAV infection to determine whether pre-infection treatment alleviated inflammation in the lungs.

## Bronchoalveolar lavage fluid and lung collection

After euthanasia using sodium pentobarbital, the primary trachea and lungs of each mouse were cannulated and flushed once with 400  $\mu$ l of phosphate-buffered saline (PBS) followed by three flushes with 300  $\mu$ l of PBS. Total and differential leukocyte counts were obtained from the resulting bronchoalveolar lavage fluid (BALF). Cell types were identified based on standard morphological criteria. Blood was removed from whole lungs by perfusion of 5 ml of PBS through the right ventricle of the heart. Then they were rapidly excised *en bloc*, rinsed in PBS, blotted, snap-frozen in liquid nitrogen, and stored at –80°C prior to further analysis.

## Lung function measurement

Invasive pulmonary function devices (pulmonary function testing systems, DSI, Holliston, U.S.A.) were used to measure lung function of the mice. Briefly, each mouse was weighed and anesthetized with an intraperitoneal injection of pentobarbital (240 mg.kg<sup>–1</sup>) (Merck, Kenilworth, U.S.A.). Fifteen minutes after the induction of anesthesia, the trachea was cannulated using an 18-G, 30-mm intravenous plastic catheter, and a suture was used to seal the wall of the trachea around the cannula. The mouse was placed into a plastic chamber that was connected to a small-animal ventilator. After the breathing of the mouse was stabilized, forced expired volume over 0.1 s (FEV0.1), forced vital capacity

(FVC), and functional residual capacity (FRC) of the lungs were measured in accordance with the manufacturer's instruction.

## Histology

The left lung lobe from each mouse was removed without airway lavage and immersed in 4% paraformaldehyde for a minimum of 24 h. For the evaluation of mean linear intercepts (MLIs) evaluation, another eight mouse lungs in each treatment group were perfusion-fixed *in situ* for 10 min using 4% paraformaldehyde at 20 cm H<sub>2</sub>O pressure via a tracheal cannula and a constant-pressure syringe pump (Harvard, Holliston, U.S.A.). The lungs were left *in situ* for 1 h, then removed and immersed in 4% paraformaldehyde for a minimum of 24 h. After fixation, the lung tissues were processed in paraffin wax. Four- $\mu$ m thick sections were cut with a microtome, mounted on glass microscope slides, processed to remove the paraffin, and stained with hematoxylin and eosin. The stained sections were viewed on a Nikon TI2-E microscope and photographed to perform tissue-scale imaging, followed by integrating the images with Nis-Elements software. The criteria used to generate inflammation scores were based on Curtis et al [32]. The composite image of each lung section was divided into nine parts, and the final score of each lung was the average score of the nine parts. MLI was also measured in nine random fields of view of each slide.

## RNA extraction and quantitative real-time PCR

Total RNA was isolated from whole lung tissues using NucleoZOL reagent (MNG, Duren, Germany). RNA (1  $\mu$ g) was reverse-transcribed into complementary DNA using HiScript<sup>®</sup> Q RT SuperMix with gDNA wiper (Vazyme, China) in according with the manufacturer's instructions. Real-time PCR analysis was conducted using the Applied Biosystem (VI A7) with ChamQ SYBR<sup>®</sup> Color qPCR Master Mix (Vazyme, China).  $\beta$ -Actin mRNA was used as an internal control. The threshold cycle (Ct) value is the PCR cycle number (out of 40) at which the measured fluorescent signal exceeds a calculated background threshold. It identifies the amplification of the target sequence value. The Ct value is proportional to the number of input target copies present in the sample. Ct numbers were transformed using  $\Delta\Delta$ Ct (threshold cycle time) and the relative value method and were expressed relative to  $\beta$ -actin mRNA levels.

## Superoxide detection

Inflammatory cells in BALF were incubated with the chemiluminescent probe L-O12 (100 mM) (Wako Chemicals, U.S.A.) in the absence (for basal measurements) or presence of the PKC and NADPH oxidase activator phorbol 12, 13 dibutyrate (PDB, 1 mM) (Sigma Aldrich). Cells were dispensed into 96-well opti-plates. Luminescence was measured with a Multiscan Spectrum (Tecan Infinite M1000pro). Photon emission was recorded for 1 s for 30 cycles. Individual datapoints for each group were averaged from two replicates, subtracted against the average background values, normalized to total cell numbers, and expressed as relative light units.

## Western blot analysis

A lysis buffer containing protease inhibitors was used to extract total protein from the frozen tissues. Protein concentrations were determined using a BCA assay kit. Proteins were separated by SDS-PAGE and transferred onto polyvinylidene difluoride membranes. The membranes were probed overnight with antibodies against  $\beta$ -actin (1:2,000 dilution, Cell Signaling Technology), heme oxygenase-1 (HO-1) (1:2,000 dilution, Abcam), and gp91 [phox] (1:2,000 dilution, BD Pharmingen). The membranes were then incubated with goat anti-rabbit or goat anti-mouse horseradish peroxidase-conjugated IgG at room temperature for 1.5 h. Immunoblots were detected and assessed using the Gel Doc XR+ Gel documentation system (Bio-rad).  $\beta$ -Actin was used as the housekeeping protein.

## Viral titration

The whole lungs were removed aseptically, placed into bottles containing 1.0 ml of PBS with penicillin (1000 U.ml<sup>-1</sup>) and streptomycin (1000  $\mu$ g.ml<sup>-1</sup>). Virus was extracted by grinding lungs followed by centrifugation. Plaques assays were performed as previously described [33]. Briefly, samples were diluted and incubated for 1 h on a Madin-Darby canine kidney (MDCK) cell monolayer to allow viral adsorption. Next, 1% agarose dissolved in MEM containing 1  $\mu$ g/ml TPCK-treated trypsin was added to cells and incubated at 37°C for 72 h. The cells were then fixed with 4% formaldehyde in saline for 1 h and stained with crystal violet. The plates were rinsed in water and plaques were counted. Viral titer was expressed as the PFU per lung.



## Cytopathic effect assay of anti-IAV activity *in vitro*

Six hundred milligrams of *JPYFII* formulation was dissolved in 10 ml of MEM to prepare a 60 mg/ml stock solution, which was shaken overnight at 37°C then filtered through a 0.22- $\mu$ m syringe filter and stored at –20°C for further use. Carboxylate oseltamivir (MW 312.4), which served as a positive agent, was purchased from Shanghai Roche Pharmaceuticals, Ltd. and dissolved in MEM at a concentration of 1 mg/ml.

A/GZ/GIRD07/09 (H1N1) and B/Lee/1940 (FluB) were isolated from patient specimens at the Guangzhou Institute of Respiratory Health, China; A/HK/Y280/97 (H9N2), A/PR/8/34 (H1N1), and A/Aichi/2/1968 (H3N2) were kindly provided by Professor Zifeng Yang (Guangzhou Institute of Respiratory Health, China). All viruses were passaged in MDCK cells or 9- to 11-day-old specific pathogen-free chick embryos (purchased from Guangdong Wenshi Dahuanong Biotechnological Co., Ltd.) in a biosafety level 2 laboratory. MDCK cells were obtained from the Cell Bank of the typical Culture Preservation Committee of the Chinese Academy of Sciences (Shanghai, China), and routinely passaged in MEM supplemented with 10% fetal bovine serum, at 37 °C, and 5% CO<sub>2</sub>.

To evaluate the antiviral activities of *JPYFII* formulation against IAV, the cytopathic effect assay was used to examine the protective effect of *JPYFII* on cell morphological changes induced by different IAV strains *in vitro*. The half-maximal inhibitory concentration (IC<sub>50</sub>) and selection index were utilized. A 90% MDCK monolayer was formed in 96-well plates, and the wells were divided into four groups: a normal group (MEM + MEM), a virus group (IVA + MEM), a positive control group (IVA + MEM with carboxylate oseltamivir), and a *JPYFII* treatment group (IVA + MEM with *JPYFII*). The cells were inoculated with 100-fold 50% tissue culture infective dose of the IAV dilution for 2 h at 37°C. After adsorption, the supernatant was discarded, and the cells were washed twice with PBS. One hundred microliters of *JPYFII* formulation at the indicated concentrations (starting with 2000  $\mu$ g/ml, >TC<sub>50</sub>, followed by multiple dilutions until a concentration of 31.25  $\mu$ g/ml was achieved) was added to the infected cells with 1.5  $\mu$ g/ml N-Tosyl-L-Phenylalanine Chloromethyl Ketone (TPCK) treated-trypsin. After a 48-h incubation at 37°C cell lesions were observed with an inverted microscope (Leica, Wetzlar, Germany), and the IC<sub>50</sub> of the *JPYFII* formulations were calculated according to the Reed-Muench method.

## Statistical analysis

Grouped data are presented and expressed as mean  $\pm$  standard error of the mean (S.E.M.). *n* represents the number of mice per treatment group. Statistical significance was determined by one-way or two-way analysis of variance (ANOVA) followed by Dunnett test or Sidak post hoc test for multiple comparisons. All statistical analyses were performed using GraphPad Prism for Windows (version 7.0). *P* < 0.05 was considered statistically significant.

## Result

### *JPYFII* formulation did not affect body weight in IAV-infected mice exposed to CS

The body weight of each mouse was measured and recorded daily to determine the effects of *JPYFII* formulation on body weight. Compared with sham + MEM + saline mice, the average body weight of CS + IAV + saline mice was slightly but significantly decreased, by 3.2% (*P* < 0.05). *JPYFII* formulation did not change the body weights of sham + MEM or CS + IAV mice (*P* > 0.05) (Figure 1).

### *JPYFII* formulation reduced the number of inflammatory cells in BALF from IAV-infected mice exposed to CS

Cellular inflammatory responses in the airways were examined by analyzing BALF from each mouse treated with either vehicle or *JPYFII* formulation (Figure 2A–E). The numbers of total cells, macrophages, neutrophils, and lymphocytes were significantly increased in BALF from CS + IAV + saline mice compared with sham + MEM + saline mice (*P* < 0.05). *JPYFII* formulation reduced the numbers of total cells, macrophages, neutrophils, and lymphocytes in BALF from CS + IAV mice. *JPYFII* formulation did not affect the numbers of total cells, macrophages, neutrophils, or lymphocytes in BALF from sham + MEM mice.

### *JPYFII* formulation alleviated airway inflammation but did not affect MLI or lung function in IAV-infected mice exposed to CS

Representative images in Figure 3A–L show hematoxylin and eosin-stained lung sections from mice treated with either vehicle or *JPYFII* formulation. Panels (A–D) depict sections of whole lung at the level of the porta pulmonis

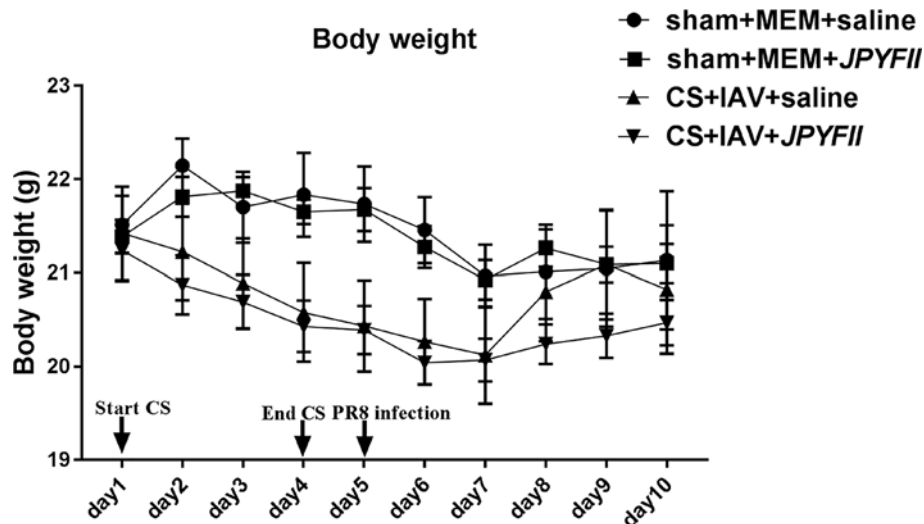


**Figure 1.** Effect of *JPYFII* formulation on body weight in CS-exposed and IAV-infected mice

Mouse body weight was recorded before oral gavage daily from day 1 to day 10. Mouse body weights are shown as average body weight within each treatment group every day and expressed as mean  $\pm$  S.E.M. for  $n = 6$  to 8 mice per treatment group.

of the left lung lobes. Panels (E–H) depict inflammatory infiltrates in alveolar, peribronchial, and perivascular areas. Panels (I–L) depict the integrity and area of the pulmonary alveoli.

CS exposure combined with IAV infection (Figure 3C) resulted in severe pulmonary consolidation and inflammatory reactions composed of perivascular, peribronchial, and alveolar infiltrates of monocytes/macrophages, neutrophils, and lymphocytes followed by prominent inflammatory cell cuffing around bronchi and in the lung parenchyma (Figure 3G).

Inflammatory scores in perivascular, peribronchial, and alveolar areas in CS + IAV + saline mice were significantly higher than those in sham + MEM + saline mice ( $P < 0.01$ ). *JPYFII* formulation reduced the area of pulmonary consolidation and inflammatory scores in alveolar regions ( $P < 0.01$ ) and peribronchial regions ( $P < 0.05$ ) in CS + IAV mice (Figure 3D,H,M,N). *JPYFII* formulation did not reduce inflammatory scores in perivascular areas in CS + IAV mice (Figure 3O). MLI, an indicator of alveolar size, was not increased in CS + MEM + saline mice compared to sham + MEM + saline mice. *JPYFII* formulation did not reduce the MLI in sham + MEM or CS + IAV mice (Figure 3P). Representative pictures are shown in Figure 3I–L.

To evaluate the effects of *JPYFII* formulation on lung function in sham + MEM + saline mice and CS + IAV + saline mice, the FRC of lungs and the ratio of FEV<sub>0.1</sub>/FVC were measured using the animal pulmonary function testing system. FRC and FEV<sub>0.1</sub>/FVC ratio did not change significantly in CS + IAV + saline mice compared with sham + MEM + saline mice. *JPYFII* formulation treatment did not reduce FRC or increase the FEV<sub>0.1</sub>/FVC ratio in CS + IAV mice (Supplementary Figure S3).

### ***JPYFII* formulation reduced mRNA expression of cytokines, chemokines, and interferons in sham + IAV mice and CS + IAV mice**

To identify which mediators were responsible for the lung inflammatory response when CS + IAV mice were treated with *JPYFII* formulation, mRNA expression levels of a panel of inflammatory cytokines, chemokines, matrix metalloproteinase-12 (*Mmp12*), and interferons (IFNs) were assessed in whole lung tissue using quantitative real-time PCR. To verify whether inflammation induced by IAV was the main target of suppression by *JPYFII* formulation, the effect of *JPYFII* formulation in CS + MEM mice and sham + IAV mice were also evaluated.

mRNA expression levels of proinflammatory chemokines (*Cxcl5*, *Cxcl10*, and *Ccl2*;  $P < 0.05$  or  $P < 0.01$ ), *Mmp12* ( $P < 0.01$ ), and IFNs (*Ifn $\beta$*  and *Ifn $\lambda$* ;  $P < 0.05$  and  $P < 0.01$ ) were significantly increased in CS + IAV + saline mice compared with sham + IAV + saline mice (Table 2). CS + IAV + saline mice also exhibited increased cytokine (*Tnf- $\alpha$* ,  $P < 0.01$ ), chemokine (*Cxcl1*, *Cxcl5*, *Cxcl10*, and *Ccl2*;  $P < 0.01$ ), *Mmp12* ( $P < 0.01$ ), and IFN (*Ifn $\alpha$* , *Ifn $\beta$* , and *Ifn $\gamma$* ;  $P < 0.05$  or  $P < 0.01$ ) mRNA expression compared with CS + MEM + saline mice.

CS + IAV mice treated with *JPYFII* formulation exhibited markedly reduced cytokine (*Il-6* and *Tnf- $\alpha$* ,  $P < 0.01$ ), and chemokine (*Cxcl1*, *Cxcl2*, *Cxcl5*, *Cxcl10*, and *Ccl2*;  $P < 0.01$ ) mRNA expression compared to CS + IAV + saline

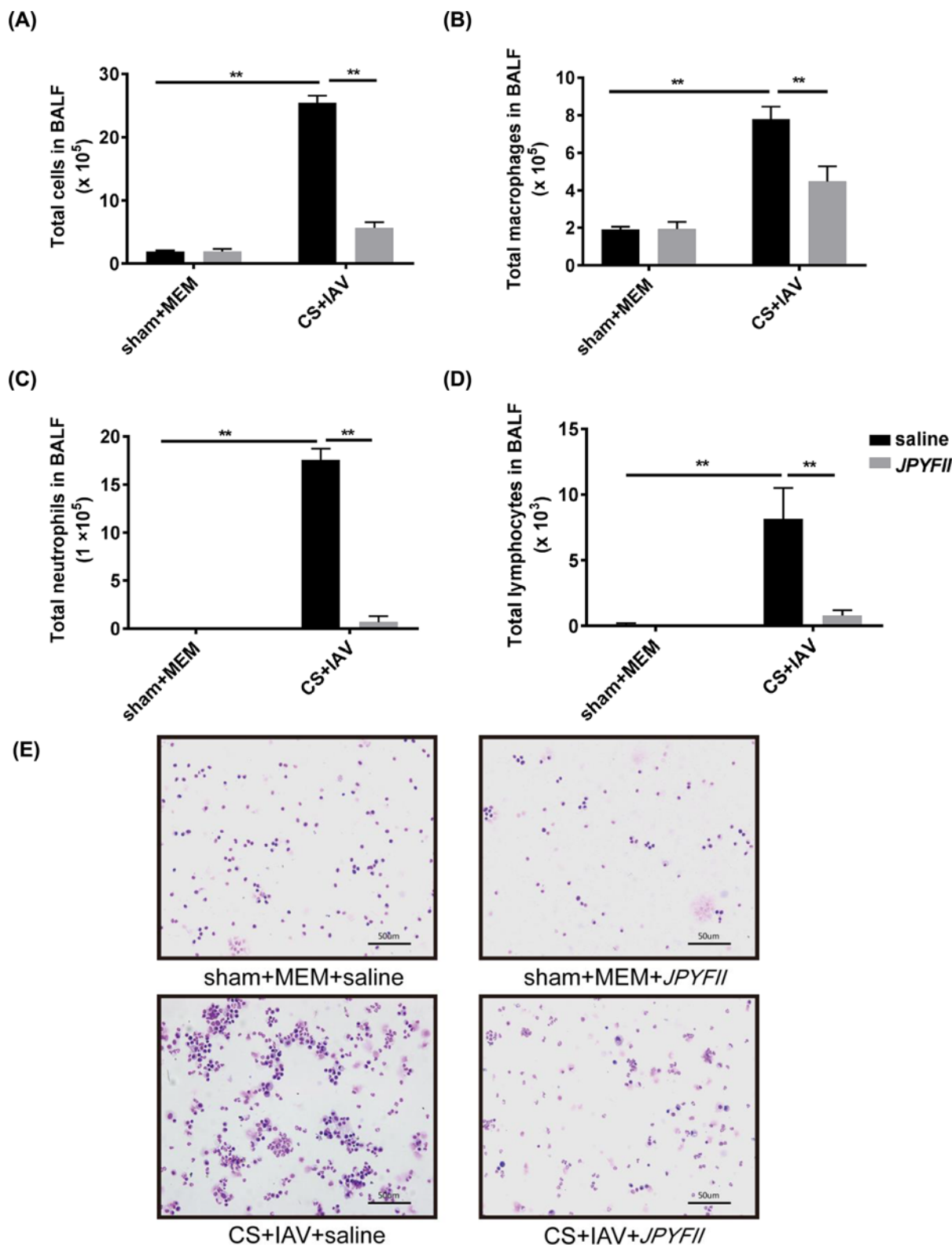


**Figure 2.** Effect of JPYFII formulation on total cells, neutrophils, macrophages and lymphocytes in CS-exposed and IAV-infected mice

BALF cellularity is shown as the total population of cells (A), macrophages (B), neutrophils (C), and lymphocytes (D). Representative Diff Quik-stained cytopsin preparations of BALF from mice in each treatment group (E). Data are expressed as mean  $\pm$  S.E.M for  $n = 6-8$  per treatment group. Two-way ANOVA with Sidak post-hoc test was performed to assess statistical significance;  $**P < 0.01$ .

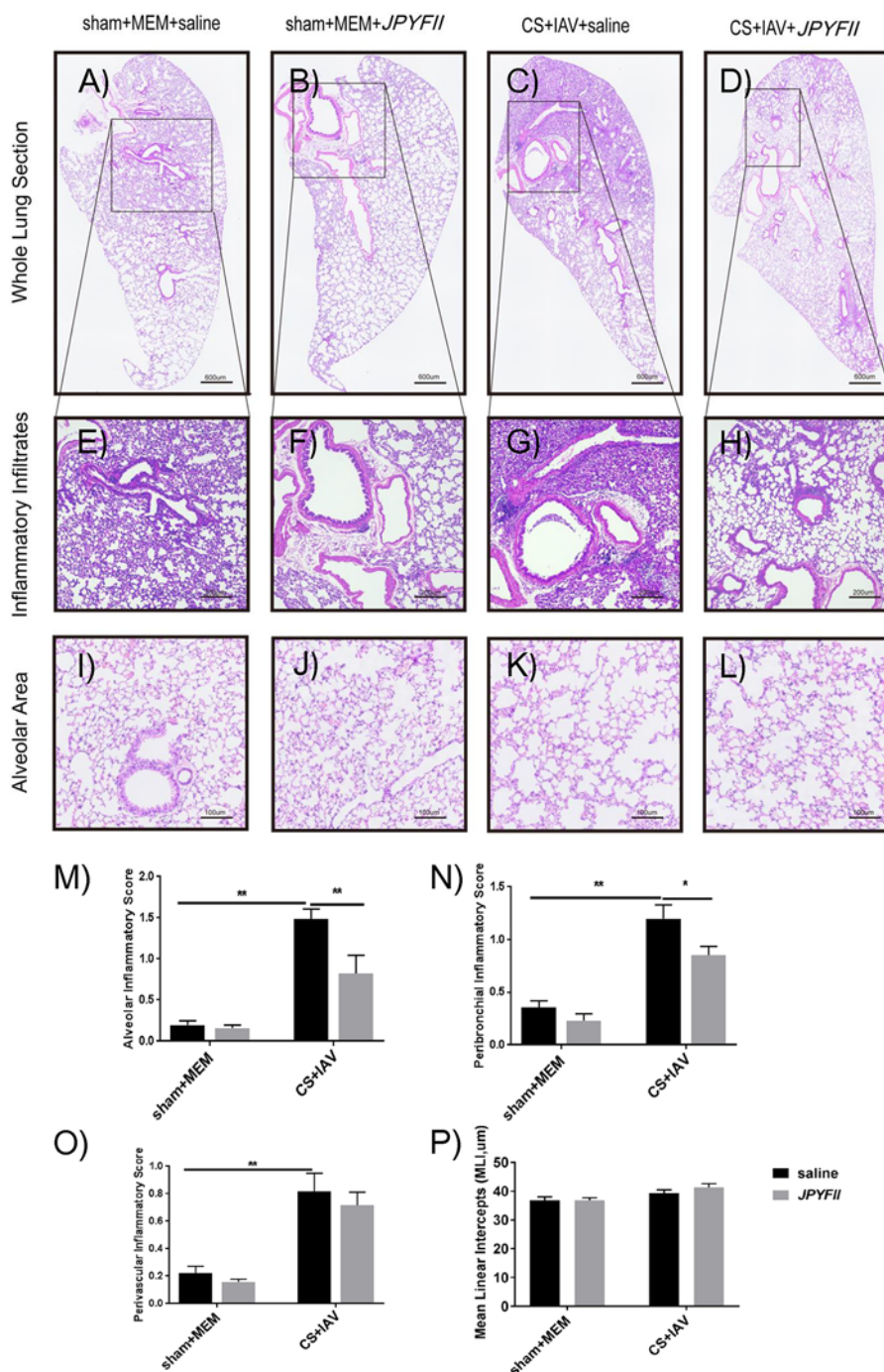


**Figure 3. Effect of *JPYFII* formulation on histopathology of lungs exposed to CS and infected with IAV**

H&E stained lung sections from mice euthanized on day 5 after IAV infection. The top four sections (A–D) illustrate representative composite images at the level of the porta pulmonis of the left lung lobes of sham + MEM mice (A), sham + MEM + *JPYFII* mice (B), CS + IAV mice (C), and CS + IAV + *JPYFII* mice (D). The lower four sections (E–H) show the inflammatory infiltrates in lungs of sham + MEM mice (E), sham + MEM + *JPYFII* mice (F), CS + IAV mice (G), and CS + IAV + *JPYFII* mice (H). The last four sections (I–L) illustrate the integrity and area of the pulmonary alveoli in sham + MEM mice (I), sham + MEM + *JPYFII* mice (J), CS + IAV mice (K), and CS + IAV + *JPYFII* mice (L). The sections are magnified 100 $\times$  for E–H and 200 $\times$  for (I–L). The scale bar (lower right corner of all figures) denotes 600  $\mu$ m for (A–D), 200  $\mu$ m for (E–H), and 100  $\mu$ m for (I–L). The inflammatory score was evaluated in the alveolar (M), peribronchial (N) and perivascular areas (O), and MIL (P) was also measured and shown in this figure. Data are shown as mean  $\pm$  S.E.M for  $n=9$  mice. Statistical significance was assessed using two-way ANOVA with Sidak post hoc test; \* $P < 0.05$ , \*\* $P < 0.01$ .



**Table 2** Effect of *JPYFII* administration on whole lung cytokine, chemokine, and protease mRNA expression in control, CS-exposed, IAV-infected, and IAV-induced CS exposed mice

Gene	sham + MEM + Sali	sham + MEM + <i>JPYFII</i>	sham + IAV + Sali	sham + IAV + <i>JPYFII</i>	CS + MEM + Sali	CS + MEM + <i>JPYFII</i>	CS + IAV + Sali	CS + IAV + <i>JPYFII</i>
<b>Cytokines</b>								
<i>Il-6</i>	1.08 ± 0.22	0.67 ± 0.15	76.33 ± 42.34**	18.59 ± 27.21▲▲	0.28 ± 0.06*	0.29 ± 0.07	50.32 ± 14.37**	3.34 ± 2.68△△
<i>Tnf-α</i>	1.09 ± 0.42	0.59 ± 0.09	1.29 ± 0.44	1.32 ± 0.43	0.17 ± 0.05	0.07 ± 0.04	3.56 ± 0.66***	1.11 ± 0.31△△
<i>Il-1β</i>	0.95 ± 0.28	0.84 ± 0.33	2.78 ± 1.15	1.64 ± 0.7	0.73 ± 0.15	1.54 ± 0.53	3.59 ± 1.39*	1.45 ± 0.79
<b>Chemokines</b>								
<i>Cxcl1</i>	1.00 ± 0.10	1.17 ± 0.36	11.42 ± 3.73**	3.59 ± 2.1▲	0.49 ± 0.33	0.26 ± 0.05	13.56 ± 1.26***	2.00 ± 0.64△△
<i>Cxcl2</i>	0.87 ± 0.16	1.06 ± 0.31	16.74 ± 4.65**	5.97 ± 2.47▲▲	0.31 ± 0.08	0.29 ± 0.07	12.79 ± 2.34**	1.66 ± 0.50△△
<i>Cxcl5</i>	1.02 ± 0.17	0.59 ± 0.15	1.80 ± 0.59	0.50 ± 0.16	0.10 ± 0.03	0.02 ± 0.005	10.51 ± 2.05**▲▲##	1.86 ± 0.51△△
<i>Cxcl10</i>	1.06 ± 0.39	0.49 ± 0.10	3.44 ± 0.81	1.51 ± 0.48	0.16 ± 0.04	0.08 ± 0.07	19.76 ± 5.10**▲▲##	1.49 ± 0.87△△
<i>Ccl2</i>	0.88 ± 0.25	0.86 ± 0.22	12.76 ± 4.22	4.30 ± 2.53	0.47 ± 0.43	0.22 ± 0.14	30.61 ± 9.26**▲▲##	6.28 ± 5.35△△
<b>Proteases</b>								
<i>Mmp12</i>	0.93 ± 0.13	0.79 ± 0.21	0.45 ± 0.12	0.21 ± 0.07	0.47 ± 0.44**	0.22 ± 0.14	1.55 ± 0.18▲▲##	0.87 ± 0.28
<b>Interferons</b>								
<i>Ifn-α</i>	1.10 ± 0.40	0.44 ± 0.09	1.05 ± 0.67	0.71 ± 0.18	0.18 ± 0.05	0.09 ± 0.08	2.03 ± 0.96#	0.92 ± 0.30
<i>Ifn-β</i>	0.82 ± 0.11	0.65 ± 0.19	1.23 ± 0.76	0.63 ± 0.15	0.14 ± 0.04	0.07 ± 0.06	3.05 ± 0.62**▲##	1.45 ± 0.63
<i>Ifn-γ</i>	1.06 ± 0.25	0.92 ± 0.17	3.36 ± 0.96*	1.17 ± 0.24▲	0.27 ± 0.08	0.13 ± 0.03	5.45 ± 2.04***	1.63 ± 0.57
<i>Ifn-λ</i>	0.91 ± 0.09	0.67 ± 0.12	12.79 ± 4.0**	2.20 ± 0.74▲▲	0.27 ± 0.08	0.12 ± 0.03	3.81 ± 0.91**▲▲	1.04 ± 0.37

Gene expression was measured simultaneously under identical conditions using quantitative real-time PCR. Responses are shown as fold changes relative to sham + MEM + saline mice after normalization to the expression of the house-keeping gene,  $\beta$ -actin. Data are shown as the mean ± S.E.M. for triplicate reactions of 6–8 individual mouse lungs. Two-way ANOVA with Sidak post hoc test was performed to assess statistical significance. \* $P < 0.05$  and \*\* $P < 0.01$  versus the sham + MEM + Saline group; # $P < 0.05$  and ## $P < 0.01$  versus the CS + MEM + Saline group; ▲ $P < 0.05$ , ▲▲ $P < 0.01$  versus the sham + IAV + Saline group; △ $P < 0.05$ , △△ $P < 0.01$  versus the CS + IAV + Saline group.

mice (Table 2). *JPYFII* formulation significantly reduced cytokine (*Il-6*,  $P < 0.01$ ), chemokine (*Cxcl1* and *Cxcl2*,  $P < 0.05$  and  $P < 0.01$ ), and IFN (*Ifnγ* and *Ifnλ*,  $P < 0.05$  and  $P < 0.01$ ) mRNA expression in sham + IAV mice. *JPYFII* formulation did not reduce the expression of any of the above mediators in CS + MEM mice.

## ***JPYFII* formulation alleviated superoxide production in BALF cells**

Excessive oxidative stress is one of the main features of the lungs in patients with COPD and AECOPD [18]. To determine whether *JPYFII* formulation alleviated oxidative stress in the lungs of CS + IAV + saline mice, superoxide production was measured in BALF cells, and HO-1 and gp91 levels were measured in lung tissue. The production of superoxide from BALF cells was assessed *ex vivo* under PDB-stimulated conditions. Superoxide was significantly increased in CS + IAV + saline mice compared with sham + MEM + saline mice (7,218.68 ± 2,512.57 and 49.96 ± 15.18 respectively;  $P < 0.01$ ). In contrast, *JPYFII* formulation blocked excessive production of superoxide in CS + IAV + saline mice (169.12 ± 141.15;  $P < 0.01$ ) (Figure 4A). Compared with sham + MEM + saline mice, protein levels of gp91 and HO-1 in mice exposed to CS + IAV were significantly increased, by 2.31-fold and 2.13-fold respectively ( $P < 0.05$ ). Administration of *JPYFII* formulation decreased the expression of both gp91 (1.35 ± 0.20;  $P < 0.01$ ; Figure 4B,C) and HO-1 (1.22 ± 0.12;  $P < 0.01$ ) in CS + IAV mice compared with the saline control group (Figure 4B,D). *JPYFII* formulation did not significantly alter superoxide production (61.91 ± 87.30;  $P > 0.05$ ) or protein expression of gp91 (0.95 ± 0.15;  $P > 0.05$ ) or HO-1 (1.05 ± 0.07;  $P > 0.05$ ) in sham + MEM mice.

Superoxide production was assessed in BALF cells from sham + IAV + saline mice, sham + IAV + *JPYFII* mice, CS + MEM + saline mice, and CS + MEM + *JPYFII* mice. Superoxide was significantly increased in sham + IAV + saline mice compared with sham + MEM + saline mice ( $P < 0.01$ ), and superoxide levels were reduced by 57% ( $P > 0.05$ ) after *JPYFII* formulation treatment. CS exposure did not increase superoxide levels in the lungs of sham + MEM mice (Supplementary Figure S4).

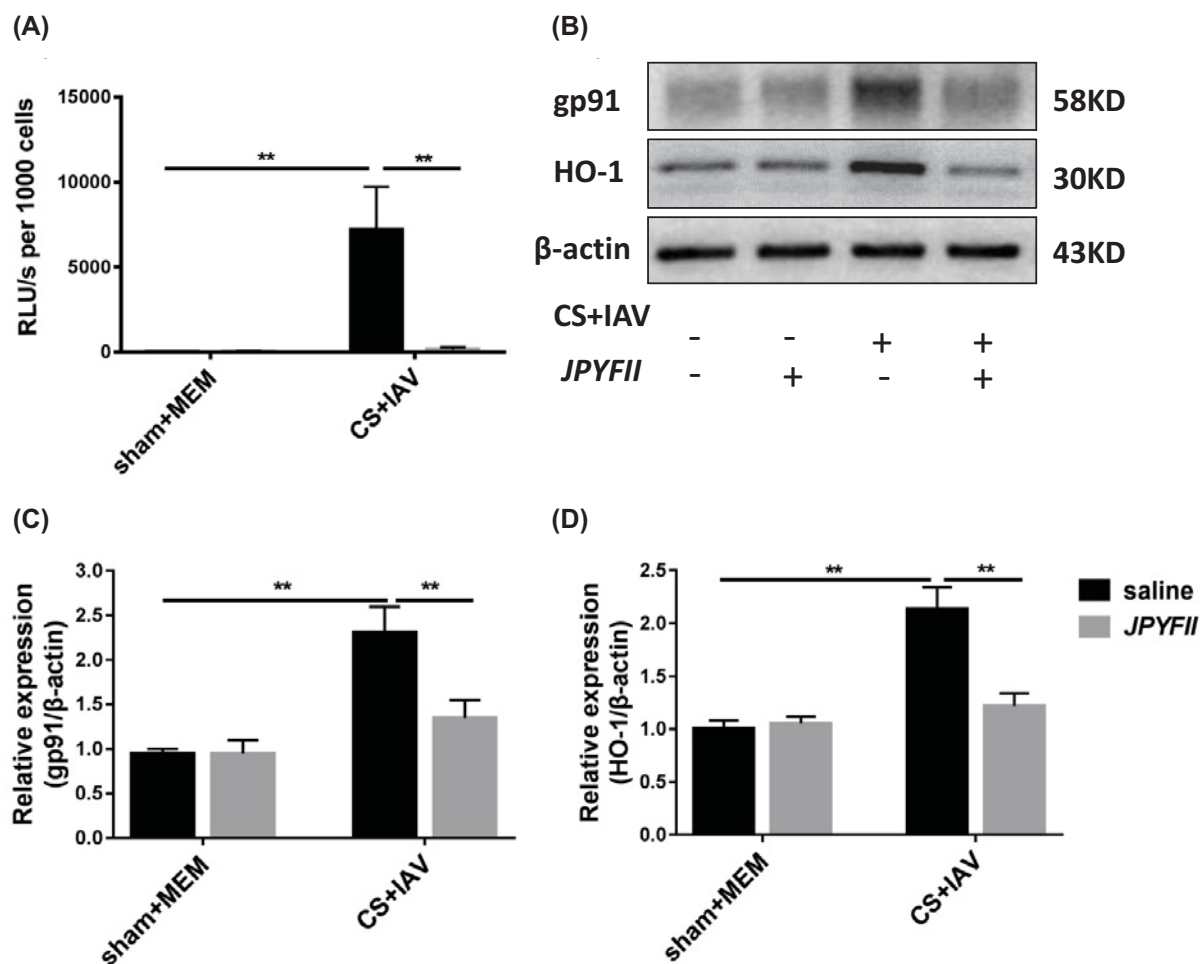


**Figure 4. Effect of *JPYFII* formulation on oxidative stress in lungs of mice exposed to CS and infected with IAV**

Reactive oxygen species production from BALF cells was assessed *ex vivo* under PDB-stimulated conditions (A). Relative light units (RLU)/second per 1,000 cells was calculated. Protein expression of gp91 and HO-1 in lung tissue was assessed using Western blot and representative bands were shown (B). The intensity of each band was adjusted according to the value of the background and normalized to β-actin housekeeping protein. Data are shown as mean ± S.E.M for  $n = 14$ –16 mice (C and D). Statistical significance was assessed using two-way ANOVA with Sidak post hoc test; \*\* $P < 0.01$ .

### ***JPYFII* formulation reduced load of IAV *in vivo* and *in vitro***

To determine whether suppression of inflammation and reactive oxygen species production by *JPYFII* formulation was due to viral clearance, we examined viral load, expression of IAV nucleoprotein in mouse lungs, and the antiviral effects of *JPYFII* formulation *in vitro*. Viral titer ( $36.86 \pm 7.83$  PFU/lung;  $P < 0.01$ ) and IAV nucleoprotein ( $415.03 \pm 57.11$ ;  $P < 0.01$ ) were significantly increased in CS + IAV + saline mice compared with sham + MEM + saline mice ( $0.00 \pm 0.00$  and  $1.00 \pm 0.33$ , respectively) (Figure 5A–C). *JPYFII* formulation treatment significantly reduced viral titer ( $11.67 \pm 5.76$  PFU/lung;  $P < 0.01$ ) and nucleoprotein ( $23.80 \pm 23.31$ ;  $P < 0.01$ ) expression at the mRNA level in CS + IAV mice.

Analysis of antiviral effects of *JPYFII* formulation using a cytopathic effect assay (Table 3) indicated that *JPYFII* formulation inhibited replication of A/GZ/GIRD07/09 (H1N1) ( $IC_{50} 296.19 \pm 1.59$ ), A/PR/8/34 (H1N1) ( $IC_{50} 325.95 \pm 15.51$ ), A/Aichi/2/1968 (H3N2) ( $IC_{50} 349.31 \pm 31.37$ ), and A/HK/Y280/97 (H9N2) ( $IC_{50} 682.44 \pm 32.08$ ) in MDCK cells. *JPYFII* formulation did not inhibit replication of the B/Lee/1940 (FluB) strain ( $IC_{50} > 1200$ ) *in vitro*.

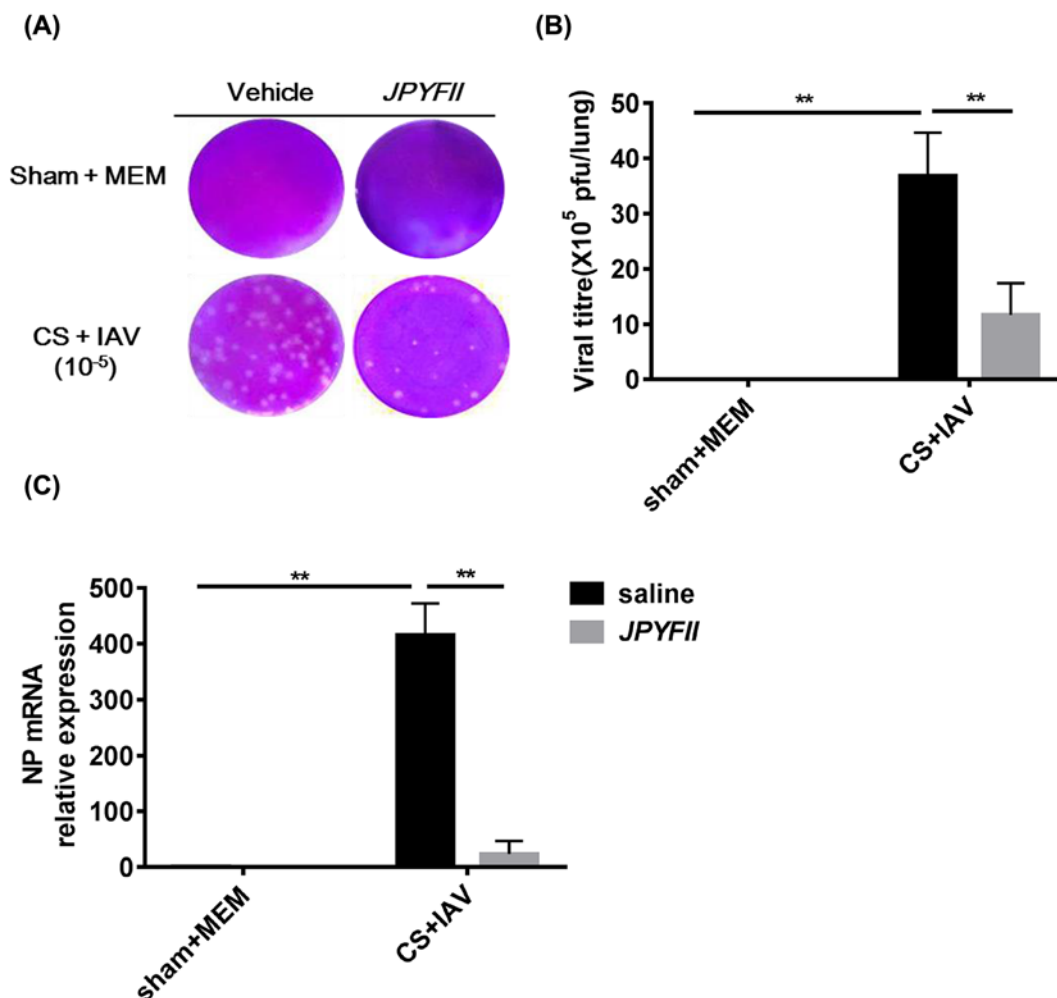


**Figure 5.** Effect of JPYFII formulation on viral load in lungs of mice exposed to CS and infected with IAV

Viral titers were determined using plaque assays of individual lung homogenates in MDCK cells,  $n = 6-8$  per group (A and B). mRNA expression of NP (C) was measured with qPCR. Data was showed as mean  $\pm$  S.E.M for  $n = 6-8$  mice. Two-way ANOVA with Sidak post hoc test was performed to assess statistical significance;  $**P < 0.01$ .

**Table 3** Inhibition activity of JPYFII formulation on different strains of virus

Strains	Inhibition activity of JPYFII formulation ( $\mu\text{g/ml}$ )			Carboxylate oseltamivir ( $\mu\text{g/ml}$ )		
	TC <sub>50</sub>	IC <sub>50</sub>	SI	TC <sub>50</sub>	IC <sub>50</sub>	SI
A/PR/8/34(H1N1)	1198.67 $\pm$ 62.73	325.95 $\pm$ 15.51	3.69 $\pm$ 0.37	>2000	0.51 $\pm$ 0.05	>100
A/GZ/GIRD07/09(H1N1)	1198.67 $\pm$ 62.73	296.19 $\pm$ 1.59	4.05 $\pm$ 0.19	>2000	0.45 $\pm$ 0.03	>100
A/Aichi/2/1968(H3N2)	1198.67 $\pm$ 62.73	349.31 $\pm$ 31.37	3.44 $\pm$ 0.13	>2000	3.62 $\pm$ 0.13	>100
A/HK/Y280/97(H9N2)	1198.67 $\pm$ 62.73	682.44 $\pm$ 32.08	1.76 $\pm$ 0.01	>2000	2.86 $\pm$ 0.06	>100
B/Lee/1940(FluB)	1198.6 $\pm$ 62.73	>1200	<1	>2000	12.6 $\pm$ 1.87	>100

Inhibition activity of JPYFII formulation on different strains of H1N1, H3N2, H9N2, and FluB was detected by CPE assay. IC<sub>50</sub>, TC<sub>50</sub>, and SI are described to evaluate the toxicity and inhibitory activity of JPYFII formulation. SI is equal to the ratio of TC<sub>50</sub> and IC<sub>50</sub>. SI > 2 indicates that the tested medicine is highly effective and low toxic. 1 < SI < 2 indicates that the tested medicine has low effectiveness and is highly toxic. SI < 1 indicates the medicine is not effective. Data are shown as the mean  $\pm$  S.E.M. from triplicate tests.

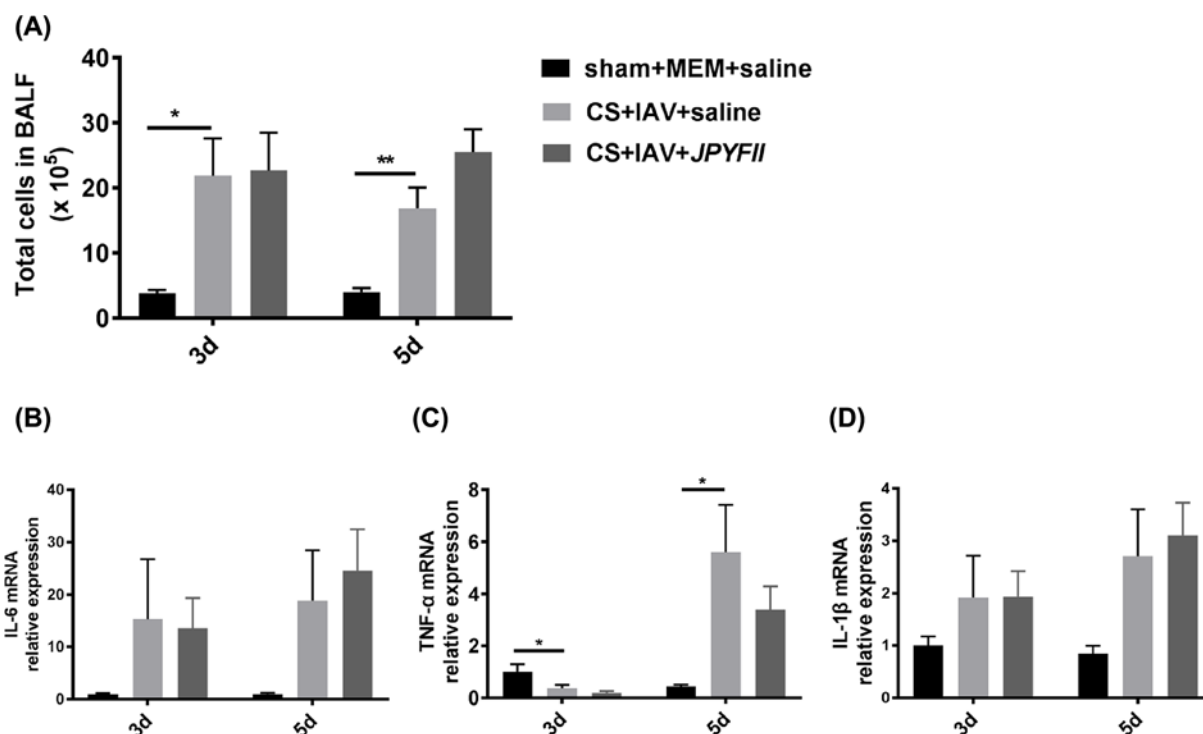


**Figure 6. Effect of pre-infection treatment with *JPYFII* formulation on CS-exposed and IAV-infected mice**

BALF cellularity is shown as the total population of cells (A), *Tnf- $\alpha$*  (B), *Il-6* (C), and *Il-1 $\beta$*  (D) mRNA expression in whole lung are shown as fold-change relative to saline treated sham + MEM + saline mice after normalization to  $\beta$ -actin house-keeping mRNA expression. Data are shown as the mean  $\pm$  S.E.M. for  $n = 6$ –7 mouse lungs. One-way ANOVA with Dunnett test was performed to assess statistical significance; \* $P < 0.05$ , \*\* $P < 0.01$ .

## Pre-infection treatment with *JPYFII* formulation did not alleviate inflammation in lung

We have previously reported that *JPYFII* formulation alleviated inflammation and oxidative stress in CS-exposed mice [34], suggesting that it could provide protective effects against CS exposure. Given that CS worsened influenza virus (PR8 strain)-induced lung inflammation in a previous study [16], we hypothesized that *JPYFII* formulation treatment during CS exposure may reduce inflammation in CS + IAV-infected mice by protecting the epithelium from CS exposure.

Pre-infection treatment with *JPYFII* formulation did not reduce the numbers of BALF cells on day 3 ( $22.67 \pm 5.80 \times 10^5$ ;  $P > 0.05$ ) or day 5 ( $25.53 \pm 3.47 \times 10^5$ ;  $P > 0.05$ ) after IAV infection compared with CS + IAV + saline mice ( $21.90 \pm 5.73 \times 10^5$  on day 3;  $16.85 \pm 3.22 \times 10^5$  on day 5, Figure 6A). Pre-infection treatment with *JPYFII* formulation did not decrease the expression of IL-6 mRNA ( $13.62 \pm 5.76$  on day 3;  $24.58 \pm 7.89$  on day 5), TNF- $\alpha$  mRNA ( $0.19 \pm 0.08$  on day 3;  $3.38 \pm 0.90$  on day 5), or IL-1 $\beta$  mRNA ( $1.93 \pm 0.49$  on day 3;  $3.10 \pm 0.63$  on day 5) compared with CS + IAV + saline mice (Figure 6B–D).

## Discussion

Airway inflammation is one of the characteristic pathological changes observed in CS and infection-induced diseases (i.e., AECOPD). Both CS and viral infections lead to lung inflammatory responses, which include recruitment of immune cells into the airway, the release of proinflammatory cytokines, and an oxidant–antioxidant imbalance [35–37]. Infection with respiratory pathogens such as rhinovirus, influenza virus, and coronavirus reportedly aggravates inflammation in CS-exposed lungs [38,39]. Thus, resolution of inflammation is essential for the successful treatment of respiratory virus-associated AECOPD. In the present study, we investigated mice exposed to CS and infected with IAV to mimic the airway inflammation that occurs in AECOPD. *JPYFII* formulation reduced inflammatory cell influx and infiltration in the lungs, as well as expression of proinflammatory cytokines, chemokines, and oxidative stress in BALF cells and lungs in CS + IAV mice. It also reduced viral amounts *in vivo* and *in vitro*. Notably however, *JPYFII*



formulation treatment prior to IAV infection did not reduce airway leukocyte influx or the release of proinflammatory cytokines in the lungs of CS + IAV mice.

In patients with AECOPD and animals challenged with IAV and CS, the inflammatory cell population in airways is increased [40,41]. Neutrophilia and lymphocythemia are indicators of an acute inflammatory response, especially in virus-associated conditions [42]. CS induces increased neutrophils and macrophages [43]. The leukocyte recruitments described above are usually driven by chemokines such as *Cxcl1* and *Cxcl2* among others, which are released by injured pulmonary epithelium [44]. In the present study *JPYFII*-treated CS + IAV mice exhibited fewer leukocytes, macrophages, neutrophils, and lymphocytes, indicating that *JPYFII* formulation alleviated inflammatory responses in the airways. This result was supported by histology observations indicating that *JPYFII* formulation reduced the infiltration of inflammatory cells, especially neutrophils and lymphocytes, in peribronchial and alveolar areas of the lungs in CS + IAV mice. The area of pulmonary consolidation was reduced in the CS + IAV mice that received *JPYFII* formulation treatment. These results indicated that *JPYFII* formulation facilitated the resolution of inflammation in the IAV-induced and CS-exposed lungs.

The mechanisms by which *JPYFII* formulation suppressed inflammatory cell influx in the lungs were investigated. The influx of immune cells into lungs depends on regulation by chemoattractants. *Cxcl1* and *Cxcl5*, which are mainly expressed in epithelium, are neutrophilic chemokines [45] and were significantly increased in the CS + IAV mice. *Ccl2*, *Cxcl2*, and *Cxcl10*, the chemokines which recruit lymphocytes and monocytes, were also increased in CS + IAV mouse lungs. Therefore, increased expression of the chemokines in the lung tissue may explain the observed increases in macrophages, lymphocytes, and neutrophils that followed CS exposure and influenza infection. *JPYFII* formulation significantly reduced expression of *Cxcl1*, *Cxcl2*, *Cxcl5*, *Cxcl10*, and *Ccl2* in CS + IAV mouse lungs but not sham + MEM mouse lungs. Thus, the *JPYFII* formulation may have reduced the number of leukocytes induced by CS combined with IAV by down-regulating the expression of chemoattractants.

Expression of chemokines was regulated transcriptionally via inflammatory pathways [46,47]. Blocking toll-like receptor (TLR) 2 or inhibiting MAPK and JAK/STAT pathway has been shown to suppress expression of *Cxcl1*, *Cxcl5*, and *Cxcl8* [48]. Studies have shown that the ATF6 signaling pathway, which is activated by endoplasmic reticulum stress, is involved in the regulation of *Cxcl1* [49]. In a previous study *JPYFII* formulation suppressed reticulum stress in cigarette smoke extract (CSE)-treated BEAS-2B cells [34], indicating that *JPYFII* formulation may down-regulate the expression of chemokines, for example *Cxcl1*, by dampening reticulum stress in CS + IAV mice.

*Il-6* and *Tnf- $\alpha$*  are important inflammatory mediators that are involved in acute inflammatory flare ups [50]. *Tnf- $\alpha$* , along with granulocyte-macrophage colony-stimulating factor can activate neutrophils and regulate neutrophil survival via the NF $\kappa$ B and JAK/STAT signaling pathway [51]. In the present study *Il-6* and *Tnf- $\alpha$*  mRNA expression were reduced in CS + IAV mice after *JPYFII* formulation treatment, demonstrating that the acute inflammatory response was suppressed by *JPYFII* formulation treatment. The underlying mechanism may be associated with inhibition of NF $\kappa$ B signaling pathway, which has been proved to be a target of *JPYFII* formulation in a CS+LPS mouse model [24]. Proinflammatory mediators were also detected in sham + IAV mice and CS + MEM mice with or without *JPYFII* formulation treatment. *JPYFII* formulation decreased *Il-6*, *Tnf- $\alpha$* , and *Il-1 $\beta$*  expression in sham+IAV mice, but did not affect expression of pro-inflammatory mediators in CS + MEM mice. These results demonstrated that the production of inflammatory mediators induced by IAV might be an important target in *JPYFII* formulation treatment.

Hypermetabolism induced by inflammation is one of the reasons for body-weight loss [52]. However, the body weight loss was not reduced in *JPYFII* treated CS + IAV mice compared with sham + MEM mice. As reported, nicotine in CS has a great effect on appetite suppression [53]. Thus, the data demonstrated that *JPYFII* formulation suppressed the inflammation in lungs of CS+IAV mice but did not alleviate the suppression of appetite by nicotine.

Excessive production of superoxide is a feature of AECOPD. To determine whether *JPYFII* formulation reduced oxidative stress in the lungs and investigate the mechanism involved, superoxide production was measured in BALF cells. gp-91 protein is a subunit of NADPH oxidase 2. Heme oxygenase-1 (HO-1), which can protect epithelium and endothelium from excessive oxidative stress induced by CS [54,55], and gp91 protein expression was also measured in the present study. Superoxide production, and the expression of gp-91 were significantly reduced by *JPYFII* formulation in CS + IAV-infected mice. NADPH oxidase 2 is a main superoxide generating enzyme expressed in lungs. gp91-deficient mice reportedly exhibit reduced production of superoxide radicals and decreased levels of lung inflammation after IAV infections [56,57]. Thus *JPYFII* formulation-induced reduction of superoxide and inflammation in lungs may be related to its effect on reduction of Nox2 expression. HO-1 is regulated by NRF2 and the transcription regulator protein BACH1 [58]. Down-regulation but not up-regulation of HO-1 in the lungs of CS + IAV mice treated with *JPYFII* formulation supported the speculation that *JPYFII* formulation suppressed superoxide production instead of protecting lung tissue from endogenous superoxide via the NRF2 pathway.

Viral infection leads to oxidative stress in lung tissue, and anti-oxidative stress is an important target that can be used to improve the viral clearance [57,59]. *JPYFII* formulation could reduce superoxide production in both sham + IAV mice ( $P > 0.05$ , Supplementary Figure S4) and CS + IAV mice (Figure 4A). As well as *JPYFII* formulation reducing inflammatory cells and mediators, it is possible that *JPYFII* clears influenza virus in the lungs. In the present study *JPYFII* formulation decreased viral load and expression of IAV nucleoprotein in CS + IAV mice. In *in vitro* experiments *JPYFII* formulation reduced H1N1, H3N2, and H9N2 viral loads.

Reduction of  $H_2O_2$  production weakens suppression of the expression of type I IFNs mediated by the TLR7/TLR3 signaling pathway [60,61]. Therefore, we speculated that *JPYFII* formulation may increase the expression of IFNs. However, *JPYFII* formulation did not increase the expression of *Ifn $\alpha$*  or *Ifn $\beta$*  in CS + IAV mice or sham + MEM mice. On the contrary, *JPYFII* formulation reduced the expression of IFNs (*Ifn $\alpha$* , *Ifn $\beta$* , *Ifn $\gamma$* , and *Ifn $\lambda$* ) in sham + IAV mice and CS + IAV mice. These results indicated that clearance of IAV by *JPYFII* formulation may not be dependent on IFN-related mechanism.

IFNs can contribute to a general antiviral response via the activation of a broad range of effector molecules [62]. DAT is a small-molecule compound that can augment type I IFN signaling. In a recent study treatment with DAT prior to IAV infection yielded better protection against death than DAT treatment post-IAV infection [63]. Notably, human interferon inducible transmembrane protein 3 inhibited IAV-induced inflammation [64]. These studies demonstrated that drugs that increase the expression of IFNs can prevent viral infections and inflammation induced by them. In the present study *JPYFII* treatment prior to IAV infection did not reduce inflammation in the lungs of CS + IAV mice, which is circumstantial evidence that clearance of IAV by *JPYFII* formulation is not dependent on augmentation of IFNs.

Drugs that inhibit viral replication in host cells can decrease viral loads after viral infection. Quercetin 3'-glucuronide (Q3G) is a derivative of quercetin in *Radix astragali*, and it reportedly exhibits strong binding affinity to the cap-binding site of the PB2 subunit responsible for viral replication [65]. Thus, inhibition of IAV replication may be the underlying mechanism by which *JPYFII* reduces the amount of IAV in CS-exposed mice.

One limitation of the present study is that we could not determine whether *JPYFII* formulation could improve lung function or protect structure of alveoli in CS + IAV mice. This is because 4 days of smoke exposure is too short to induce airway narrowing or destruction of the airways. Four days of smoke exposure did induced abnormal immune responses however, similar to that which occurs in COPD lungs, as has been reported in a previous study [30,66]. The effects of CS can persist after smoking cessation [16]. In the present study 4 days of CS exposure suppressed the expression of IFNs (Type I, Type II and Type III) by 71–84% of the amount observed in sham mice 5 days after smoke exposure was stopped, which was because CS reduced IFN levels by disrupting TLR3 cleavage [67,68]. In previous studies prior CS exposure has exacerbated lung inflammation in influenza virus-infected mice [59]. In the present study, there was more expression of chemokines and *Mmp12* in CS + IAV mice than in sham + IAV mice, which is concordant with a previous study [59]. We used a mouse model of CS exposure combined with IAV to evaluate the anti-inflammatory and anti-viral effects of *JPYFII* formulation. By using this experimental model, we revealed the potential benefit of *JPYFII* formulation on CS and IAV-induced inflammatory disease, *i.e.*, AECOPD.

The reason why CS aggravates influenza virus-induced inflammation is still unclear. CS exposure reportedly leads to increased neutrophilic inflammation in the airways, and delayed viral clearance due to a reduced respiratory syncytial virus-specific CD8+ T cell response [69]. In another study mice exposed to CS recovered poorly from primary Influenza A pneumonia with reduced type I and II IFNs and virus-specific immunoglobulins [70]. Thus, the underlying mechanism may be related to down-regulation of immune responses to viruses induced by CS. In the present study, CS exposure did not induce the expression of acute inflammatory cytokines because CS exposure had been stopped for 5 days by the time the lung tissue was taken. Even so, expression of chemokines and IFNs was reduced in CS + MEM mice ( $P > 0.05$ ; Table 2), which indicates persistent suppression of immune system by CS. Pre-treatment with *JPYFII* formulation did not relieve IAV-induced airway inflammation in CS + IAV mice, indicating that *JPYFII* formulation may not improve the immunosuppression induced by CS. This speculation was supported by the observation that *JPYFII* did not increase expression of chemokines or IFNs in CS + MEM mice (Table 2).

## Conclusion

In the present study, *JPYFII* formulation reduced airway inflammation in IAV-infected CS-exposed mice. Thus, the study suggests that *JPYFII* formulation may be a potential drug for the effective treatment of AECOPD associated with IAV infection.

## Clinical perspectives

- Respiratory viral infections are a common trigger of acute exacerbations of chronic obstructive pulmonary disease (COPD) and lead to severe comorbidities. Currently there is no effective antiviral therapy for patients with COPD. *Jianpiyifei II (JPYFII)* formulation, a traditional herbal formulation that includes potential antiviral components, is used to treat COPD and has anti-inflammatory effects in a smoke-exposed animal model. The present study investigated whether *JPYFII* formulation could alleviate lung inflammation in influenza A virus (IAV)-infected and cigarette smoke-exposed mice.
- In the present study *JPYFII* formulation reduced lung inflammation and oxidative stress in IAV-induced and cigarette smoke-exposed mice. The beneficial effects were largely attributed to the clearance of IAV by *JPYFII* formulation.
- The current study suggests that *JPYFII* formulation may be a useful drug for the effective treatment of acutely exacerbated COPD associated with IAV infection.

## Data Availability

The authors confirm that the data supporting the findings of this study are available within the article and its supplementary materials.

## Competing Interests

The authors declare that there are no competing interests associated with the manuscript.

## Funding

This research was supported by the National Natural Science Foundation of China [grant numbers 81573895, 81603554, 82074343, and 82074370] and Team Project in High-Level University [grant number 2021xk27].

## CRedit Author Contribution

**Xuhua Yu:** Investigation, Writing—original draft, Writing—review and editing. **Tiantian Cai:** Data curation, Writing—original draft. **Ziyao Liang:** Investigation. **Qiuling Du:** Investigation, Writing—review and editing. **Qi Wang:** Writing—review and editing. **Zifeng Yang:** Writing—review and editing. **Ross Vlahos:** Writing—review and editing. **Lei Wu:** Conceptualization, Supervision, Funding acquisition, Writing—review and editing. **Lin Lin:** Conceptualization, Funding acquisition, Writing—review and editing.

## Abbreviations

AECOPD, acute exacerbation of COPD; BALF, bronchoalveolar lavage fluid; COPD, chronic obstructive pulmonary disease; CPE, cytopathic effect; CS, cigarette smoke; Ct, threshold cycle; FRC, functional residual capacity; IAV, influenza A virus; IC50, 50% inhibitory concentration; LPS, lipopolysaccharide; MLI, mean linear intercepts; qPCR, quantitative real-time PCR; RLU, relative light units; SGRQ, St. George's Respiratory Questionnaire; SI, selection index; TC50, 50% toxic concentration.

## References

- 1 Rabe, K.F. and Watz, H. (2017) Chronic obstructive pulmonary disease. *Lancet* **389**, 1931–1940, [https://doi.org/10.1016/S0140-6736\(17\)31222-9](https://doi.org/10.1016/S0140-6736(17)31222-9)
- 2 Mathioudakis, A.G., Janssens, W., Sivapalan, P., Singanayagam, A., Dransfield, M.T., Jensen, J.S. et al. (2020) Acute exacerbations of chronic obstructive pulmonary disease: in search of diagnostic biomarkers and treatable traits. *Thorax* **75**, 520–527, <https://doi.org/10.1136/thoraxjnl-2019-214484>
- 3 Cho, W.-K., Lee, C.G. and Kim, L.K. (2019) COPD as a Disease of Immunosenescence. *Yonsei Med. J.* **60**, 407–413, <https://doi.org/10.3349/ymj.2019.60.5.407>
- 4 Zhou, M., Wang, H., Zeng, X., Yin, P., Zhu, J., Chen, W. et al. (2019) Mortality, morbidity, and risk factors in China and its provinces, 1990–2017: a systematic analysis for the Global Burden of Disease Study 2017. *Lancet* **394**, 1145–1158, [https://doi.org/10.1016/S0140-6736\(19\)30427-1](https://doi.org/10.1016/S0140-6736(19)30427-1)
- 5 Laribi, S., Pemberton, C.J., Kirwan, L., Nour, S., Turkdogan, K., Yilmaz, M.B. et al. (2017) Mortality and acute exacerbation of COPD: a pilot study on the influence of myocardial injury. *Eur. Respir. J.* **49**, <https://doi.org/10.1183/13993003.00096-2017>
- 6 MacIntyre, N. and Huang, Y.C. (2008) Acute exacerbations and respiratory failure in chronic obstructive pulmonary disease. *Proc. Am. Thorac. Soc.* **5**, 530–535, <https://doi.org/10.1513/pats.200707-088ET>

- 7 Guarascio, A.J., Ray, S.M., Finch, C.K. and Self, T.H. (2013) The clinical and economic burden of chronic obstructive pulmonary disease in the USA. *Clin. Outcomes Res.* **5**, 235–245
- 8 Rehman, A.U., Hassali, M.A.A., Muhammad, S.A., Harun, S.N., Shah, S. and Abbas, S. (2019) The economic burden of chronic obstructive pulmonary disease (COPD) in Europe: results from a systematic review of the literature. *Eur. J. Health Econ.*
- 9 Mannino, D.M. and Buist, A.S. (2007) Global burden of COPD: risk factors, prevalence, and future trends. *Lancet* **370**, 765–773, [https://doi.org/10.1016/S0140-6736\(07\)61380-4](https://doi.org/10.1016/S0140-6736(07)61380-4)
- 10 Singh, D., Agusti, A., Anzueto, A., Barnes, P.J., Bourbeau, J., Celli, B.R. et al. (2019) Global Strategy for the Diagnosis, Management, and Prevention of Chronic Obstructive Lung Disease: the GOLD science committee report 2019. *Eur. Respir. J.* **53**, 1900164, <https://doi.org/10.1183/13993003.00164-2019>
- 11 Guo-Parke, H., Linden, D., Weldon, S., Kidney, J.C. and Taggart, C.C. (2020) Mechanisms of Virus-Induced Airway Immunity Dysfunction in the Pathogenesis of COPD Disease, Progression, and Exacerbation. *Front. Immunol.* **11**, 1205, <https://doi.org/10.3389/fimmu.2020.01205>
- 12 Hewitt, R., Farne, H., Ritchie, A., Luke, E., Johnston, S.L. and Mallia, P. (2016) The role of viral infections in exacerbations of chronic obstructive pulmonary disease and asthma. *Therap. Adv. Respir. Dis.* **10**, 158–174, <https://doi.org/10.1177/1753465815618113>
- 13 Han, Y., Ling, M.T., Mao, H., Zheng, J., Liu, M., Lam, K.T. et al. (2014) Influenza virus-induced lung inflammation was modulated by cigarette smoke exposure in mice. *PLoS ONE* **9**, e86166, <https://doi.org/10.1371/journal.pone.0086166>
- 14 Kearley, J., Silver, J.S., Sanden, C., Liu, Z., Berlin, A.A., White, N. et al. (2015) Cigarette smoke silences innate lymphoid cell function and facilitates an exacerbated type I interleukin-33-dependent response to infection. *Immunity* **42**, 566–579, <https://doi.org/10.1016/j.immuni.2015.02.011>
- 15 Lippi, G. and Henry, B.M. (2020) Chronic obstructive pulmonary disease is associated with severe coronavirus disease 2019 (COVID-19). *Respir. Med.* **167**, 105941, <https://doi.org/10.1016/j.rmed.2020.105941>
- 16 Gualano, R.C., Hansen, M.J., Vlahos, R., Jones, J.E., Park-Jones, R.A., Deliyannis, G. et al. (2008) Cigarette smoke worsens lung inflammation and impairs resolution of influenza infection in mice. *Respir. Res.* **9**, 53, <https://doi.org/10.1186/1465-9921-9-53>
- 17 Barnes, P.J. (2017) Cellular and molecular mechanisms of asthma and COPD. *Clin. Sci. (London, England : 1979)* **131**, 1541–1558, <https://doi.org/10.1042/CS20160487>
- 18 Kirkham, P.A. and Barnes, P.J. (2013) Oxidative stress in COPD. *Chest* **144**, 266–273, <https://doi.org/10.1378/chest.12-2664>
- 19 Hikichi, M., Mizumura, K., Maruoka, S. and Gon, Y. (2019) Pathogenesis of chronic obstructive pulmonary disease (COPD) induced by cigarette smoke. *J. Thoracic Dis.* **11**, S2129–S2140, <https://doi.org/10.21037/jtd.2019.10.43>
- 20 Linden, D., Guo-Parke, H., Coyle, P.V., Fairley, D., McAuley, D.F., Taggart, C.C. et al. (2019) Respiratory viral infection: a potential “missing link” in the pathogenesis of COPD. *Eur. Respir. Rev.: An Off. J. Eur. Respir. Soc.* **28**, <https://doi.org/10.1183/16000617.0063-2018>
- 21 Tsoumakidou, M. and Siafakas, N.M. (2006) Novel insights into the aetiology and pathophysiology of increased airway inflammation during COPD exacerbations. *Respir. Res.* **7**, 80, <https://doi.org/10.1186/1465-9921-7-80>
- 22 Garrastazu, R., García-Rivero, J.L., Ruiz, M., Helguera, J.M., Arenal, S., Bonnardeux, C. et al. (2016) Prevalence of influenza vaccination in chronic obstructive pulmonary disease patients and impact on the risk of severe exacerbations. *Arch. Bronconeumol.* **52**, 88–95, <https://doi.org/10.1016/j.arbres.2015.09.001>
- 23 Lei, W., Lin, L., Yinji, X., Zhijia, S., Xue, G., Ping, H. et al. (2011) Clinical research on 178 cases of chronic obstructive pulmonary disease in the stable stage treated with Jianpi Yifei II. *J. Traditional Chinese Med.* **52**, 1465–1468
- 24 Fan, L., Chen, R., Li, L., Liang, Z., Yu, X., Huang, K. et al. (2018) Protective effect of Jianpiyifei II granule against chronic obstructive pulmonary disease via NF-κB Signaling pathway. *Evidence-Based Complement. Altern. Med.: eCAM* **2018**, 4265790, <https://doi.org/10.1155/2018/4265790>
- 25 Yang, F., Dong, X., Yin, X., Wang, W., You, L. and Ni, J. (2017) Radix Bupleuri: a review of traditional uses, botany, phytochemistry, pharmacology, and toxicology. *BioMed Res. Int.* **2017**, 7597596, <https://doi.org/10.1155/2017/7597596>
- 26 Wen, S., Huifu, X. and Hao, H. (2011) In vitro anti-influenza A H1N1 effect of extract of Bupleuri Radix. *Immunopharmacol. Immunotoxicol.* **33**, 433–437, <https://doi.org/10.3109/08923973.2010.527985>
- 27 Nile, S.H., Kim, D.H., Nile, A., Park, G.S., Gansukh, E. and Kai, G. (2020) Probing the effect of quercetin 3-glucoside from *Dianthus superbus* L against influenza virus infection- In vitro and in silico biochemical and toxicological screening. *Food Chem. Toxicol.* **135**, 110985, <https://doi.org/10.1016/j.fct.2019.110985>
- 28 Sochocka, M., Sobczyński, M., Ochnik, M., Zwolińska, K. and Leszek, J. (2019) Hampering Herpesviruses HHV-1 and HHV-2 Infection by Extract of Ginkgo biloba (EGb) and Its Phytochemical Constituents. *Front. Microbiol.* **10**, 2367, <https://doi.org/10.3389/fmicb.2019.02367>
- 29 Zou, M., Liu, H., Li, J., Yao, X., Chen, Y., Ke, C. et al. (2020) Structure-activity relationship of flavonoid bifunctional inhibitors against Zika virus infection. *Biochem. Pharmacol.* **177**, 113962, <https://doi.org/10.1016/j.bcp.2020.113962>
- 30 Yu, X., Seow, H.J., Wang, H., Anthony, D., Bozinovski, S., Lin, L. et al. (2019) Matrine reduces cigarette smoke-induced airway neutrophilic inflammation by enhancing neutrophil apoptosis. *Clin. Sci. (London, England : 1979)* **133**, 551–564, <https://doi.org/10.1042/CS20180912>
- 31 Ding, Y., Chen, L., Wu, W., Yang, J., Yang, Z. and Liu, S. (2017) Andrographolide inhibits influenza A virus-induced inflammation in a murine model through NF-κB and JAK-STAT signaling pathway. *Microbes Infect.* **19**, 605–615, <https://doi.org/10.1016/j.micinf.2017.08.009>
- 32 Curtis, J.L., Byrd, P.K., Warnock, M.L. and Kaltreider, H.B. (1991) Requirement of CD4-positive T cells for cellular recruitment to the lungs of mice in response to a particulate intratracheal antigen. *J. Clin. Invest.* **88**, 1244–1254, <https://doi.org/10.1172/JCI115428>
- 33 Liang, X., Huang, Y., Pan, X., Hao, Y., Chen, X., Jiang, H. et al. (2020) Erucic acid from *Isatis indigotica* Fort. suppresses influenza A virus replication and inflammation in vitro and in vivo through modulation of NF-κB and p38 MAPK pathway. *J. Pharmaceut. Anal.* **10**, 130–146, <https://doi.org/10.1016/j.jpha.2019.09.005>
- 34 Fan, L., Li, L., Yu, X., Liang, Z., Cai, T., Chen, Y. et al. (2020) Jianpiyifei II Granules Suppress Apoptosis of Bronchial Epithelial Cells in Chronic Obstructive Pulmonary Disease via Inhibition of the Reactive Oxygen Species-Endoplasmic Reticulum Stress-Ca(2+) Signaling Pathway. *Front. Pharmacol.* **11**, 581, <https://doi.org/10.3389/fphar.2020.00581>



- 35 Choreño-Parra, J.A., Jiménez-Álvarez, L.A., Cruz-Lagunas, A., Rodríguez-Reyna, T.S., Ramírez-Martínez, G., Sandoval-Vega, M. et al. (2021) Clinical and Immunological Factors That Distinguish COVID-19 From Pandemic Influenza A(H1N1). *Front. Immunol.* **12**, 593595, <https://doi.org/10.3389/fimmu.2021.593595>
- 36 Kovach, M.A., Che, K., Brundin, B., Andersson, A., Asgeirsdottir, H., Padra, M. et al. (2021) IL-36 Cytokines Promote Inflammation in the Lungs of Long-Term Smokers. *Am. J. Respir. Cell Mol. Biol.* **64**, 173–182, <https://doi.org/10.1165/rcmb.2020-00350C>
- 37 Zuo, L. and Wijegunawardana, D. (2021) Redox Role of ROS and Inflammation in Pulmonary Diseases. *Adv. Exp. Med. Biol.* **1304**, 187–204, [https://doi.org/10.1007/978-3-030-68748-9\\_11](https://doi.org/10.1007/978-3-030-68748-9_11)
- 38 Calvén, J., Yudina, Y., Hallgren, O., Westergren-Thorsson, G., Davies, D.E., Brandelius, A. et al. (2012) Viral stimuli trigger exaggerated thymic stromal lymphopoietin expression by chronic obstructive pulmonary disease epithelium: role of endosomal TLR3 and cytosolic RIG-I-like helicases. *J. Innate Immunity* **4**, 86–99, <https://doi.org/10.1159/000329131>
- 39 George, S.N., Garcha, D.S., Mackay, A.J., Patel, A.R., Singh, R., Sapsford, R.J. et al. (2014) Human rhinovirus infection during naturally occurring COPD exacerbations. *Eur. Respir. J.* **44**, 87–96, <https://doi.org/10.1183/09031936.00223113>
- 40 Ji, S., Bai, Q., Wu, X., Zhang, D.W., Wang, S., Shen, J.L. et al. (2020) Unique synergistic antiviral effects of Shufeng Jiedu Capsule and oseltamivir in influenza A viral-induced acute exacerbation of chronic obstructive pulmonary disease. *Biomed. Pharmacother.* **121**, 109652, <https://doi.org/10.1016/j.biopha.2019.109652>
- 41 Guo, C., Sun, X., Diao, W., Shen, N. and He, B. (2020) Correlation of Clinical Symptoms and Sputum Inflammatory Markers with Air Pollutants in Stable COPD Patients in Beijing Area. *Int. J. Chronic Obstruct. Pulmonary Dis.* **15**, 1507–1517, <https://doi.org/10.2147/COPD.S254129>
- 42 Zhang, Y., Zou, P., Gao, H., Yang, M., Yi, P., Gan, J. et al. (2019) Neutrophil-lymphocyte ratio as an early new marker in AIV-H7N9-infected patients: a retrospective study. *Therapeut. Clin. Risk Management* **15**, 911–919, <https://doi.org/10.2147/TCRM.S206930>
- 43 Yuan, F., Fu, X., Shi, H., Chen, G., Dong, P. and Zhang, W. (2014) Induction of murine macrophage M2 polarization by cigarette smoke extract via the JAK2/STAT3 pathway. *PLoS ONE* **9**, e107063, <https://doi.org/10.1371/journal.pone.0107063>
- 44 Koss, C.K., Wohnhaas, C.T., Baker, J.R., Tilp, C., Przibilla, M., Lerner, C. et al. (2021) IL36 is a critical upstream amplifier of neutrophilic lung inflammation in mice. *Commun. Biol.* **4**, 172, <https://doi.org/10.1038/s42003-021-01703-3>
- 45 Mattos, M.S., Ferrero, M.R., Kraemer, L., Lopes, G.A.O., Reis, D.C., Cassali, G.D. et al. (2020) CXCR1 and CXCR2 Inhibition by Ladarixin Improves Neutrophil-Dependent Airway Inflammation in Mice. *Front. Immunol.* **11**, 566953, <https://doi.org/10.3389/fimmu.2020.566953>
- 46 Kalchiem-Dekel, O., Yao, X., Barochia, A.V., Kaler, M., Figueroa, D.M., Karkowsky, W.B. et al. (2020) Apolipoprotein E Signals via TLR4 to Induce CXCL5 Secretion by Asthmatic Airway Epithelial Cells. *Am. J. Respir. Cell Mol. Biol.* **63**, 185–197, <https://doi.org/10.1165/rcmb.2019-02090C>
- 47 Sun, Y., Karmakar, M., Roy, S., Ramadan, R.T., Williams, S.R., Howell, S. et al. (2010) TLR4 and TLR5 on corneal macrophages regulate *Pseudomonas aeruginosa* keratitis by signaling through MyD88-dependent and -independent pathways. *J. Immunol.* **185**, 4272–4283, <https://doi.org/10.4049/jimmunol.1000874>
- 48 Tran, C.T., Garcia, M., Garnier, M., Burucoa, C. and Bodet, C. (2017) Inflammatory signaling pathways induced by *Helicobacter pylori* in primary human gastric epithelial cells. *Innate Immunity* **23**, 165–174, <https://doi.org/10.1177/1753425916681077>
- 49 Stengel, S.T., Fazio, A., Lipinski, S., Jahn, M.T., Aden, K., Ito, G. et al. (2020) Activating transcription factor 6 mediates inflammatory signals in intestinal epithelial cells upon endoplasmic reticulum stress. *Gastroenterology*, <https://doi.org/10.1053/j.gastro.2020.06.088>
- 50 Oberhoffer, M., Karzai, W., Meier-Hellmann, A., Bögel, D., Fassbinder, J. and Reinhart, K. (1999) Sensitivity and specificity of various markers of inflammation for the prediction of tumor necrosis factor- $\alpha$  and interleukin-6 in patients with sepsis. *Crit. Care Med.* **27**, 1814–1818, <https://doi.org/10.1097/00003246-199909000-00018>
- 51 Wright, H.L., Thomas, H.B., Moots, R.J. and Edwards, S.W. (2013) RNA-seq reveals activation of both common and cytokine-specific pathways following neutrophil priming. *PLoS ONE* **8**, e58598, <https://doi.org/10.1371/journal.pone.0058598>
- 52 Roubenoff, R., Roubenoff, R.A., Cannon, J.G., Kehayias, J.J., Zhuang, H., Dawson-Hughes, B. et al. (1994) Rheumatoid cachexia: cytokine-driven hypermetabolism accompanying reduced body cell mass in chronic inflammation. *J. Clin. Invest.* **93**, 2379–2386, <https://doi.org/10.1172/JCI117244>
- 53 Calarco, C.A. and Picciotto, M.R. (2020) Nicotinic Acetylcholine Receptor Signaling in the Hypothalamus: Mechanisms Related to Nicotine's Effects on Food Intake. *Nicotine & Tobacco Res.: Off. J. Soc. Res. Nicotine Tobacco* **22**, 152–163, <https://doi.org/10.1093/ntr/ntz010>
- 54 Yang, G., Li, Y., Wu, W., Liu, B., Ni, L., Wang, Z. et al. (2015) Anti-oxidant effect of heme oxygenase-1 on cigarette smoke-induced vascular injury. *Mol. Med. Rep.* **12**, 2481–2486, <https://doi.org/10.3892/mmr.2015.3722>
- 55 Wei, J., Fan, G., Zhao, H. and Li, J. (2015) Heme oxygenase-1 attenuates inflammation and oxidative damage in a rat model of smoke-induced emphysema. *Int. J. Mol. Med.* **36**, 1384–1392, <https://doi.org/10.3892/ijmm.2015.2353>
- 56 Oostwoud, L.C., Gunashinge, P., Seow, H.J., Ye, J.M., Selemidis, S., Bozinovski, S. et al. (2016) Apocynin and ebselen reduce influenza A virus-induced lung inflammation in cigarette smoke-exposed mice. *Sci. Rep.* **6**, 20983, <https://doi.org/10.1038/srep20983>
- 57 Vlahos, R., Stambas, J., Bozinovski, S., Broughton, B.R., Drummond, G.R. and Selemidis, S. (2011) Inhibition of Nox2 oxidase activity ameliorates influenza A virus-induced lung inflammation. *PLoS Pathog.* **7**, e1001271, <https://doi.org/10.1371/journal.ppat.1001271>
- 58 Chang, W.H., Thai, P., Xu, J., Yang, D.C., Wu, R. and Chen, C.H. (2017) Cigarette smoke regulates the competitive interactions between NRF2 and BACH1 for Heme Oxygenase-1 induction. *Int. J. Mol. Sci.* **18**, <https://doi.org/10.3390/ijms18112386>
- 59 Oostwoud, L.C., Gunasinghe, P., Seow, H.J., Ye, J.M., Selemidis, S., Bozinovski, S. et al. (2016) Apocynin and ebselen reduce influenza A virus-induced lung inflammation in cigarette smoke-exposed mice. *Sci. Rep.* **6**, 20983, <https://doi.org/10.1038/srep20983>
- 60 Menzel, M., Ramu, S., Calvén, J., Olejnicka, B., Sverrild, A., Porsbjerg, C. et al. (2019) Oxidative stress attenuates TLR3 responsiveness and impairs anti-viral mechanisms in bronchial epithelial cells from COPD and asthma patients. *Front. Immunol.* **10**, 2765, <https://doi.org/10.3389/fimmu.2019.02765>

- 61 To, E.E., Broughton, B.R., Hendricks, K.S., Vlahos, R. and Selemidis, S. (2014) Influenza A virus and TLR7 activation potentiate NOX2 oxidase-dependent ROS production in macrophages. *Free Radic. Res.* **48**, 940–947, <https://doi.org/10.3109/10715762.2014.927579>
- 62 Kugel, D., Kochs, G., Obojes, K., Roth, J., Kobinger, G.P., Kobasa, D. et al. (2009) Intranasal administration of alpha interferon reduces seasonal influenza A virus morbidity in ferrets. *J. Virol.* **83**, 3843–3851, <https://doi.org/10.1128/JVI.02453-08>
- 63 Steed, A.L., Christophi, G.P., Kaiko, G.E., Sun, L., Goodwin, V.M., Jain, U. et al. (2017) The microbial metabolite desaminotyrosine protects from influenza through type I interferon. *Science (New York, NY)* **357**, 498–502, <https://doi.org/10.1126/science.aam5336>
- 64 Chen, L., Zhu, L. and Chen, J. (2021) Human Interferon Inducible Transmembrane Protein 3 (IFITM3) Inhibits Influenza Virus A Replication and Inflammation by Interacting with ABHD16A. *BioMed Res. Int.* **2021**, 6652147
- 65 Gansukh, E., Nile, A., Kim, D.H., Oh, J.W. and Nile, S.H. (2020) New insights into antiviral and cytotoxic potential of quercetin and its derivatives - A biochemical perspective. *Food Chem.* **334**, 127508, <https://doi.org/10.1016/j.foodchem.2020.127508>
- 66 Jia, J., Conlon, T.M., Ballester Lopez, C., Seimetz, M., Bednorz, M., Zhou-Suckow, Z. et al. (2016) Cigarette smoke causes acute airway disease and exacerbates chronic obstructive lung disease in neonatal mice. *Am. J. Physiol. Lung Cell. Mol. Physiol.* **311**, L602–L610, <https://doi.org/10.1152/ajplung.00124.2016>
- 67 Su, Y.-C., Jalalvand, F., Thegerström, J. and Riesbeck, K. (2018) The interplay between immune response and bacterial infection in COPD: focus upon non-typeable *Haemophilus influenzae*. *Front. Immunol.* **9**, 2530, <https://doi.org/10.3389/fimmu.2018.02530>
- 68 Danov, O., Wolff, M., Bartel, S., Böhlen, S., Obernolte, H., Wronski, S. et al. (2020) Cigarette smoke affects dendritic cell populations, epithelial barrier function, and the immune response to viral infection with H1N1. *Front. Med.* **7**, 571003, <https://doi.org/10.3389/fmed.2020.571003>
- 69 Cheemarla, N.R., Uche, I.K., McBride, K., Naidu, S. and Guerrero-Plata, A. (2019) In utero tobacco smoke exposure alters lung inflammation, viral clearance, and CD8(+) T-cell responses in neonatal mice infected with respiratory syncytial virus. *Am. J. Physiol. Lung Cell. Mol. Physiol.* **317**, L212–L221, <https://doi.org/10.1152/ajplung.00338.2018>
- 70 Hong, M.J., Gu, B.H., Madison, M.C., Landers, C., Tung, H.Y., Kim, M. et al. (2018) Protective role of  $\gamma\delta$  T cells in cigarette smoke and influenza infection. *Mucosal Immunology* **11**, 894–908, <https://doi.org/10.1038/mi.2017.93>

**Figure S1** *JPYFII* formulation reduced BALF cells of CS and IAV exposed mouse in dose-dependent manner.

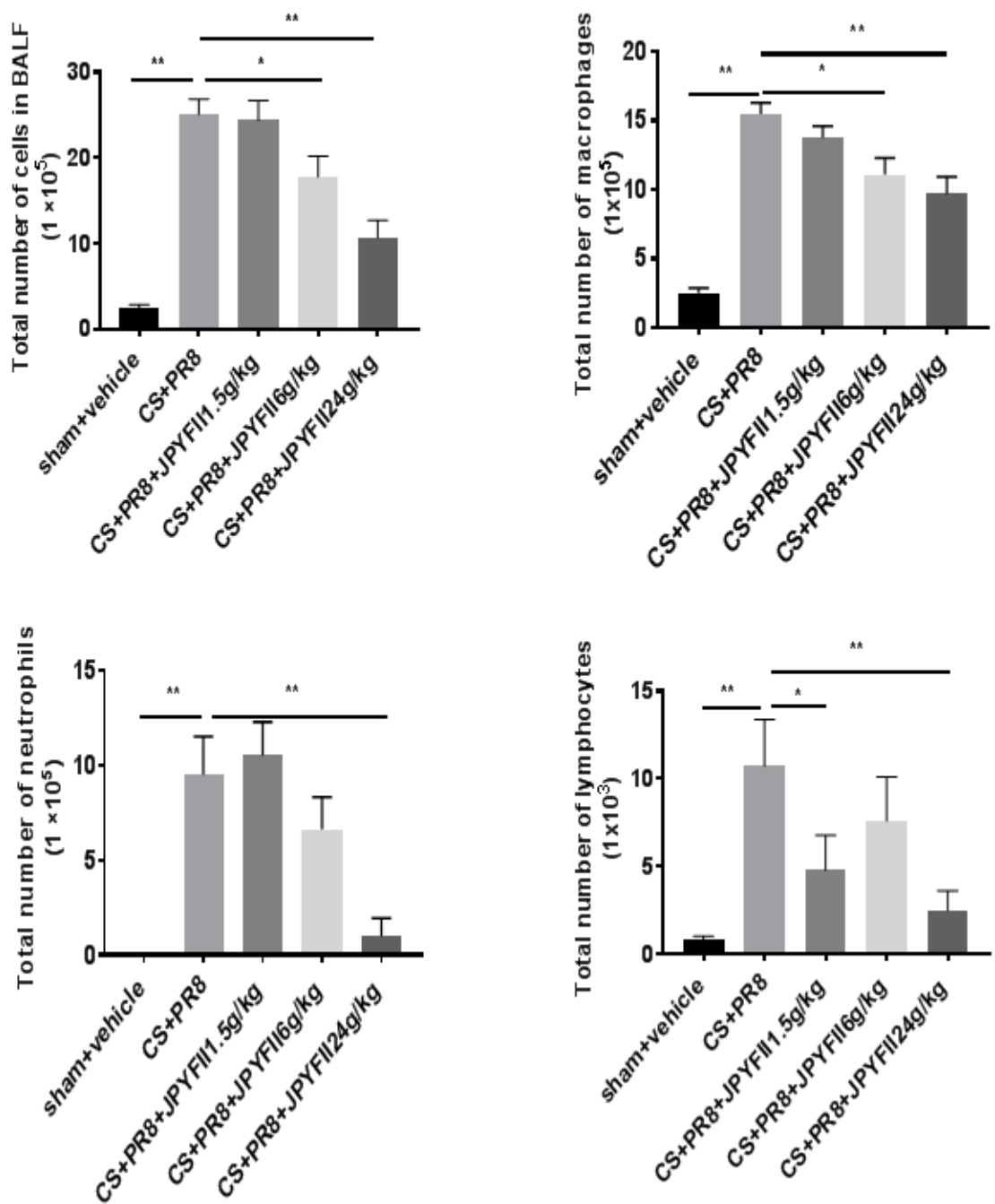


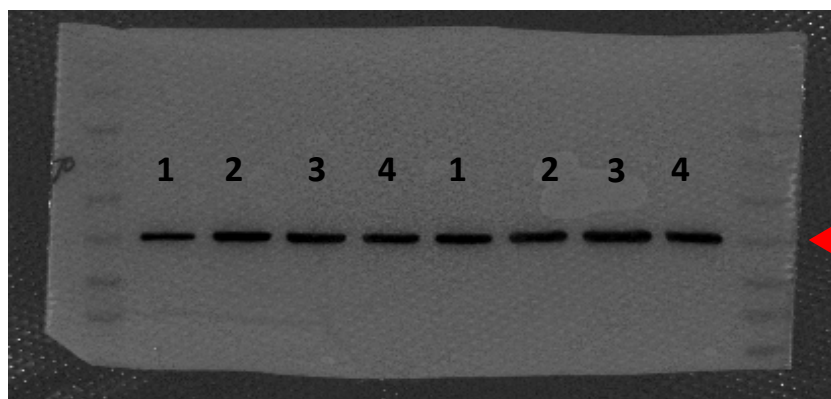
**Figure S2** *Original bands of Western blots*

**$\beta$ -actin**

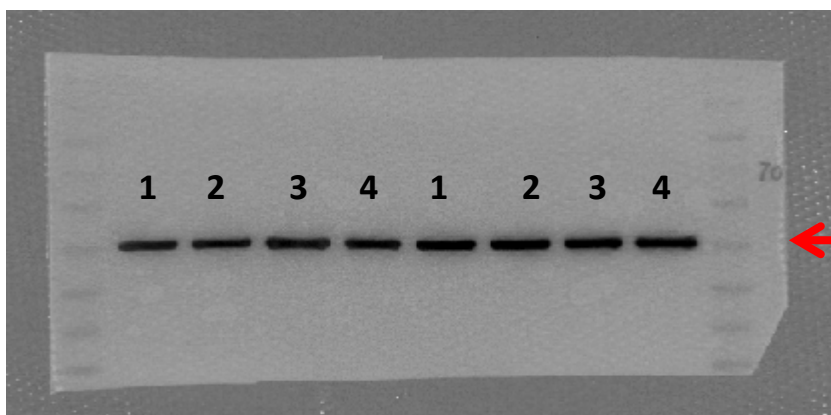
Not included in figure

Representative bands

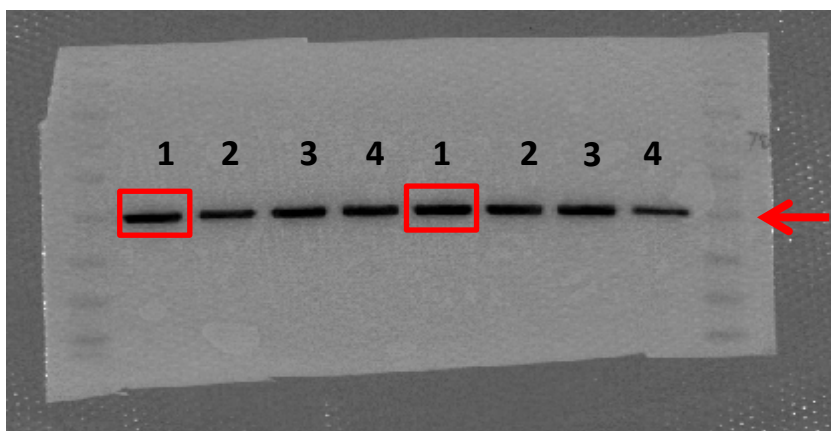
- 1 sham+MEM+saline
- 2.sham+MEM+JPFYII
- 3.CS+IAV+saline
- 4.CS+IAV+JPYFII



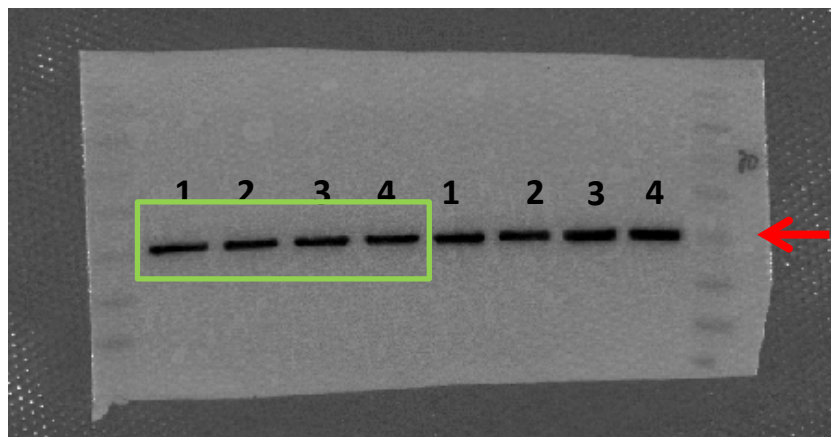
45KD



45KD



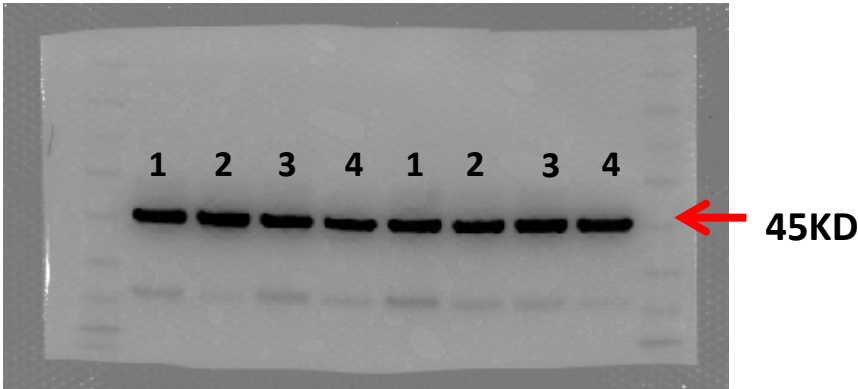
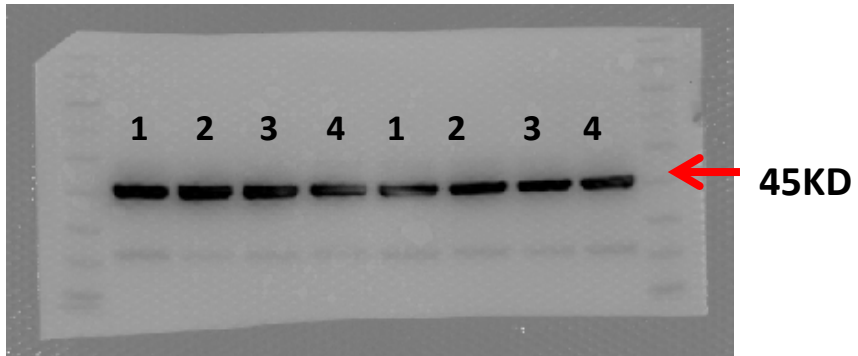
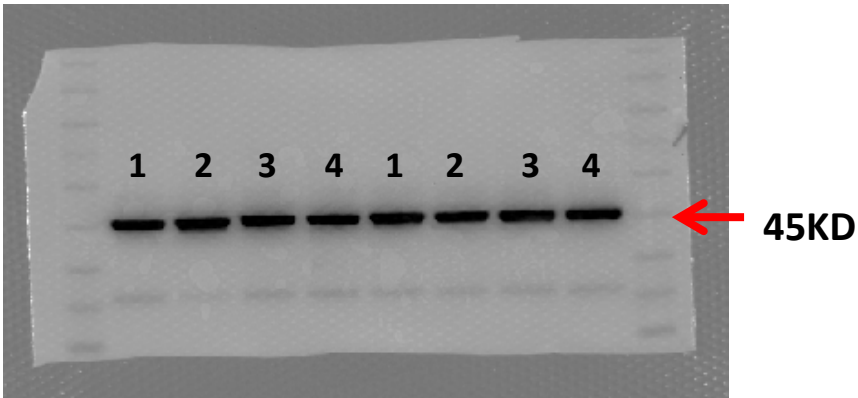
45KD



45KD



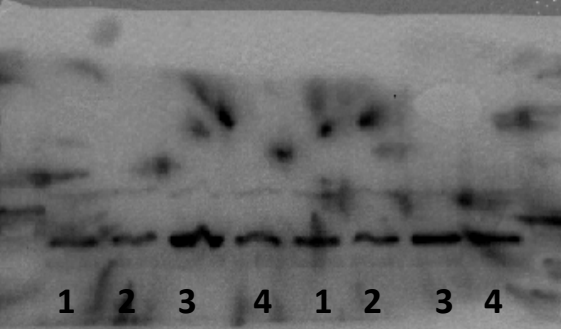
$\beta$ -actin



7c

1 2 3 4 1 2 3 4

Red arrow pointing to the bands in lane 4 of the second set.

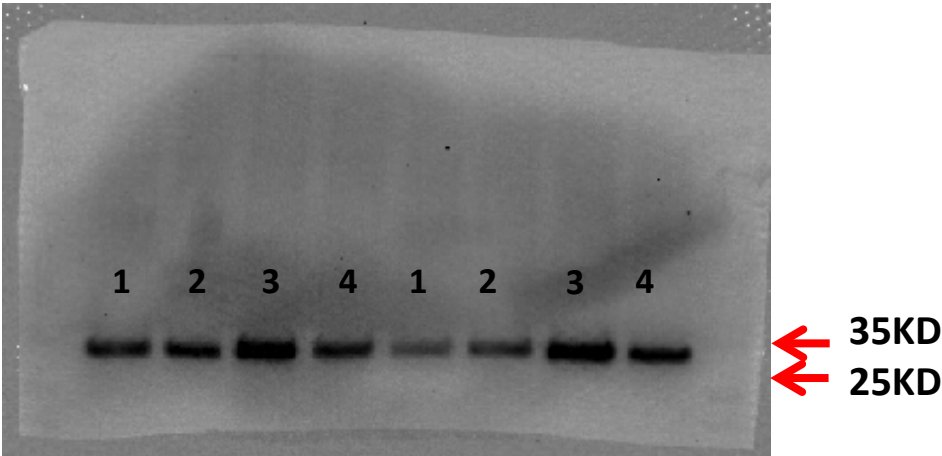
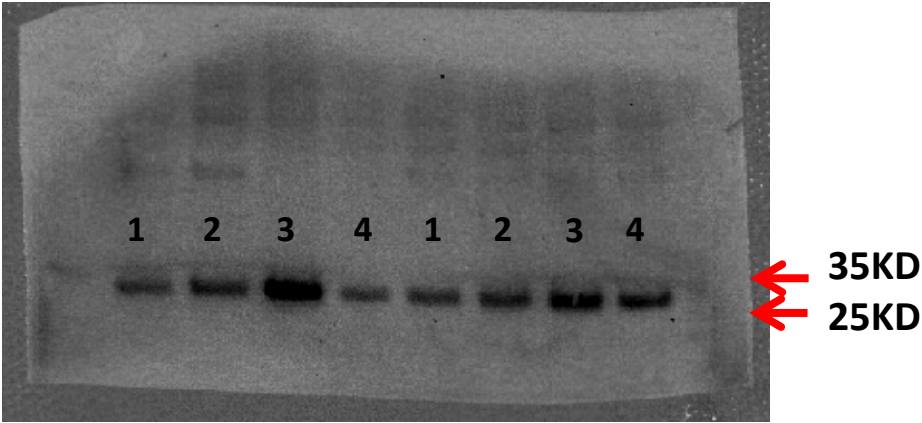
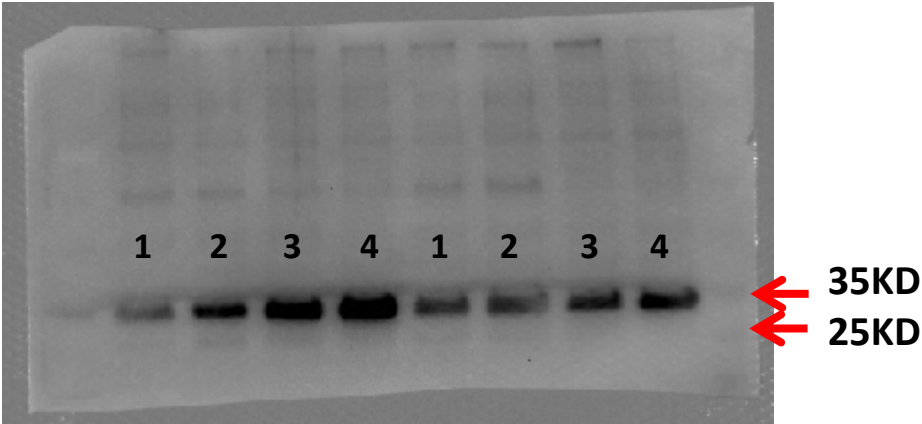
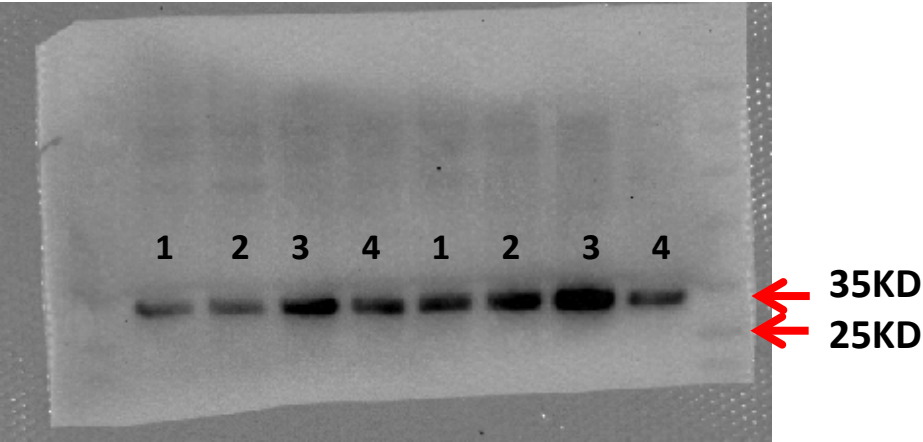


A black and white photograph of a gel electrophoresis result. The gel has two identical sets of four lanes, each labeled with the numbers 1, 2, 3, and 4. In the first set, a red box highlights a band in lane 1. In the second set, a red box highlights a band in lane 1. A red arrow points to the right, towards the second set of lanes.

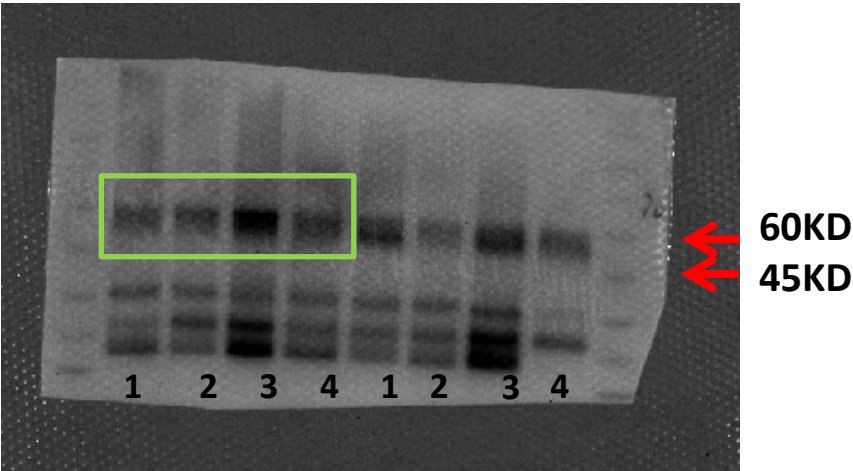
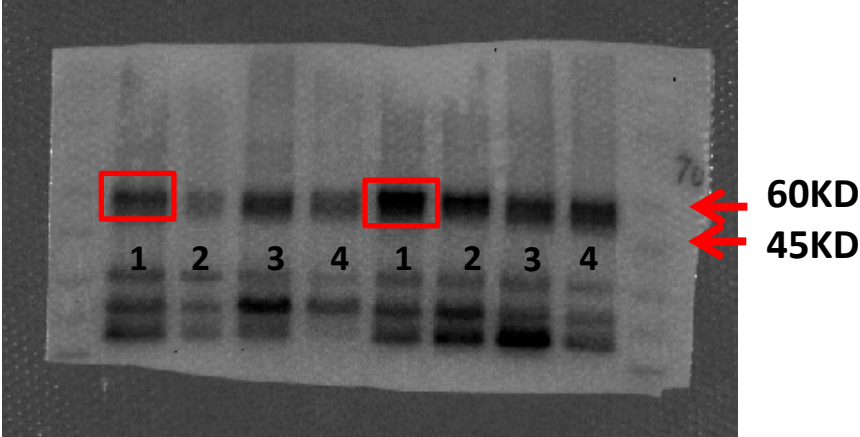
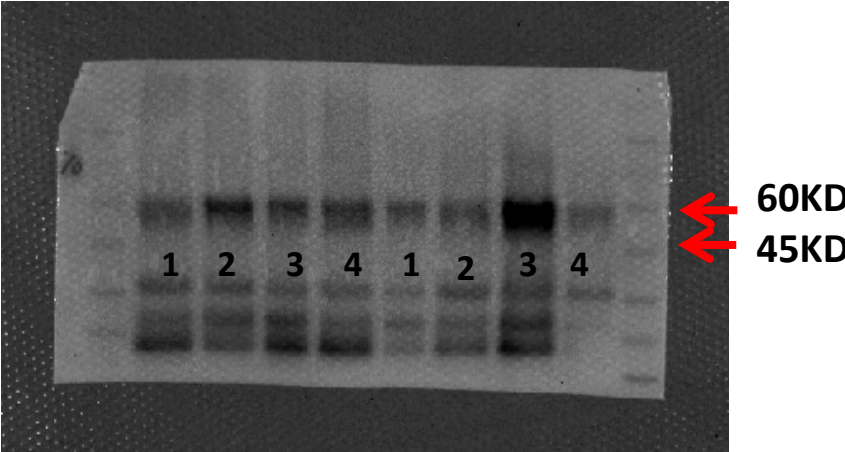
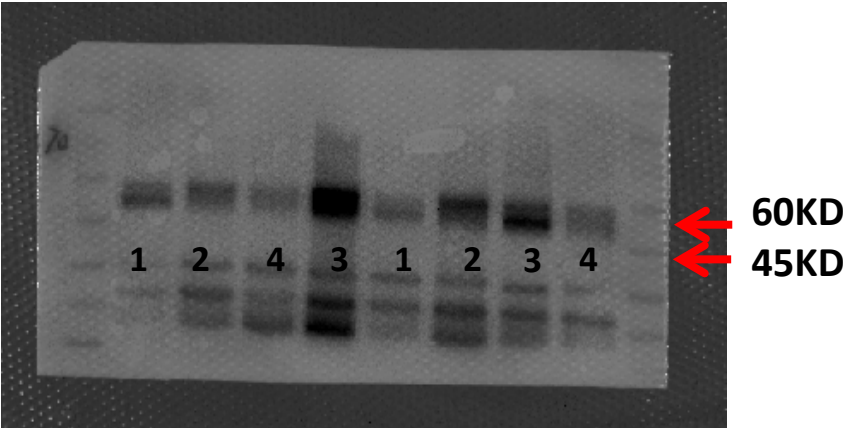


35KD  
25KD

HO-1



gp91



gp91

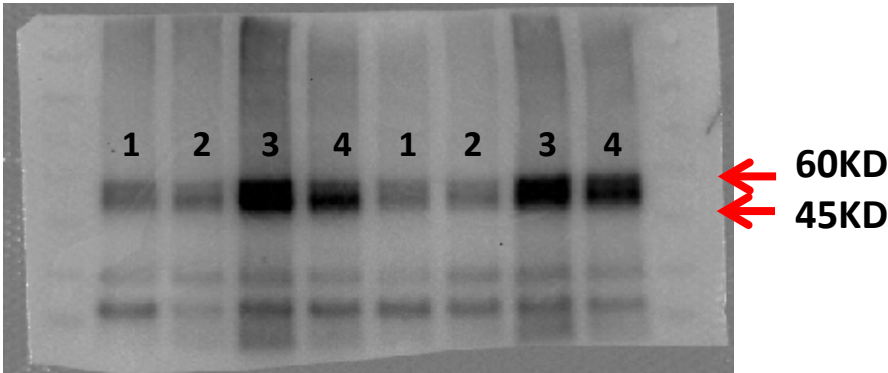
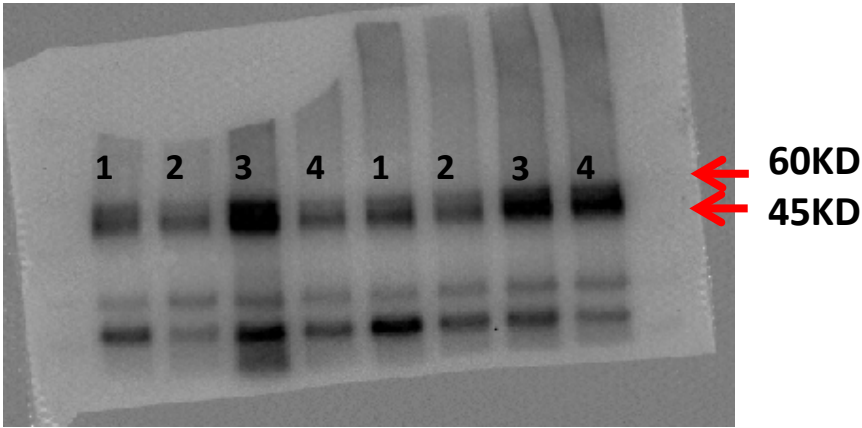
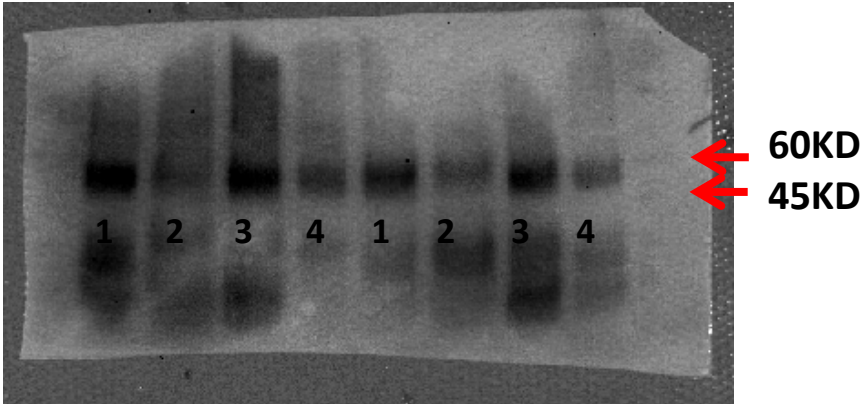
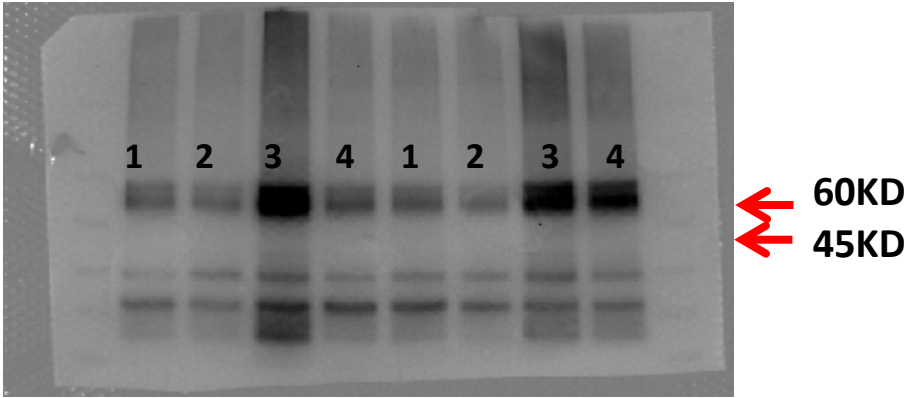




**Figure S3** Effects of *JPYFII* formulation on lung function in IAV-infected CS-exposed mice.

Lung function was assessed via the Buxco pulmonary function test. Forced vital capacity (FVC), forced expired volume over 0.1 s (FEV0.1), and functional residual capacity (FRC) in intubated BALB/c mice are shown. Data are expressed as mean  $\pm$  the standard error of the mean.  $n = 10\text{--}12$  per group.

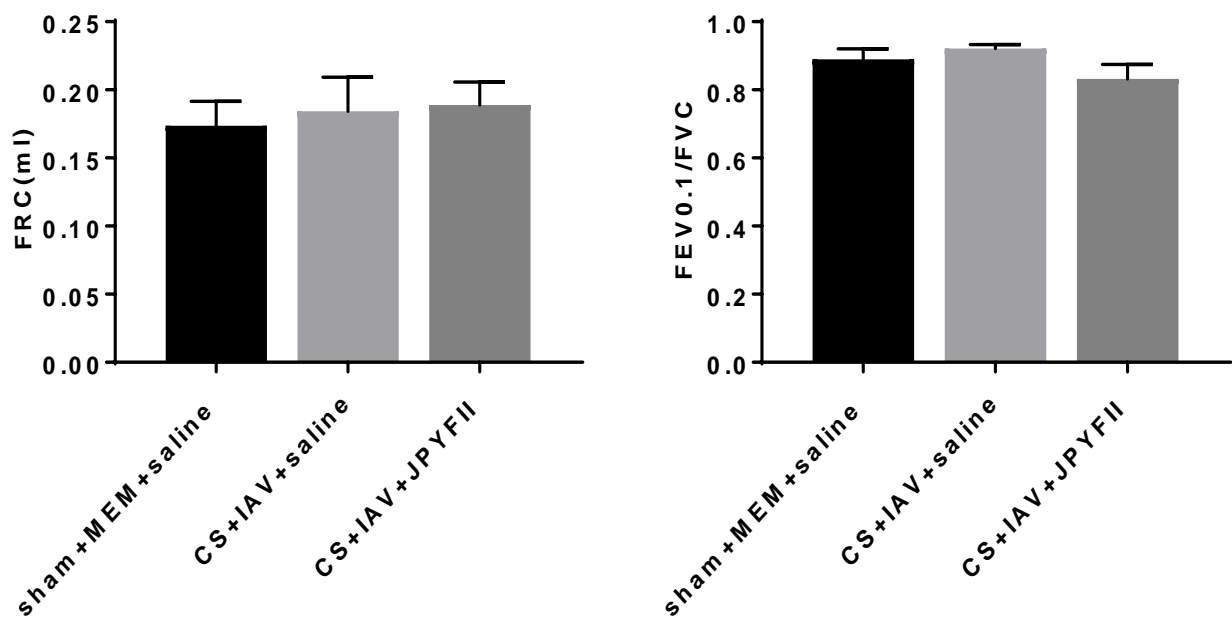


**Figure S4** Effects of *JPYFII* formulation on superoxide production in cells from BALF from the lungs of CS-exposed and IAV-infected mice.

Reactive oxygen species production from BALF cells was assessed *ex vivo* under PDB -stimulated conditions. Data are expressed as mean  $\pm$  the standard error of the mean.  $n = 6\text{--}8$  mice per group. Statistical significance was assessed using two-way analysis of variance with Tukey's test.  $**p < 0.01$

